indistinct margins ($P = 0.027$), as well as between those identified as having high and equivalent or low density ($P = 0.027$).

Comparison of mammographic findings with histological grade. Figure 3 summarizes the results of the numbers and ratios of each mammographic finding according to histological grade. There were significant differences between irregular and lobular or oval mass shape in Grade 3 ($P < 0.001$ for all). Furthermore, in Grade 1 tumors, significant differences were found between with an indistinct and microlobulated or spiculated periphery ($P = 0.030$ and $P = 0.003$), between those with spiculated and indistinct or microlobulated margins ($P < 0.001$, respectively), between those identified as high and equivalent or low density ($P = 0.047$), and between those with a linear and amorphous calcification shape ($P = 0.027$).

Comparison of mammographic findings with lymphovascular invasion. Figure 4 summarizes the results for the numbers and ratios of each mammographic finding according to lymphovascular invasion. There were significant differences between oval and irregular or round mass shape ($P = 0.008$ and $P = 0.034$), between microlobulated and indistinct periphery ($P = 0.014$), between punctate and amorphous or pleomorphic calcification shape ($P = 0.030$ and 0.038), and between presence and absence of architectural distortion ($P = 0.027$).

Comparison of mammographic findings with the Ki-67 labeling index. Figure 5 summarizes the results of correlations between mammographic findings and the Ki-67 labeling index. The Ki-67 labeling index according to mass shape was 15.74 ± 6.21 for irregular masses, 38.82 ± 13.10 for lobular masses, 36.22 ± 15.75 for oval masses, and 37.85 ± 14.95 for round masses. According to mass periphery, the Ki-67 labeling index was 35.80 ± 28.51, 34.56 ± 29.76, 11.73 ± 10.86, and 27.50 ± 24.75 for tumors with indistinct, microlobulated, spiculated, and "other" margins, respectively. For tumors with a high and equivalent or low mass density, Ki-67 labeling index was 27.68 ± 26.75 and 13.14 ± 14.10, respectively. Tumors that showed amorphous, punctate, pleomorphic, and linear calcification had a Ki-67 labeling index of 24.55 ± 7.58, 26.00 ± 18.27, 24.68 ± 9.43, and 16.00 ± 17.23, respectively. In tumors without and with architectural distortion, the Ki-67 labeling index was 22.27 ± 8.64 and 25.02 ± 7.43, respectively. There were significant differences between irregular and lobular or round ($P < 0.001$ and $P = 0.014$), spiculated and indistinct or microlobulated ($P < 0.001$ for all), and high and equivalent or low density ($P = 0.018$) groups. A trend for a positive correlation was detected between irregular and oval mass shape, but the difference did not reach statistical significance ($P = 0.062$).

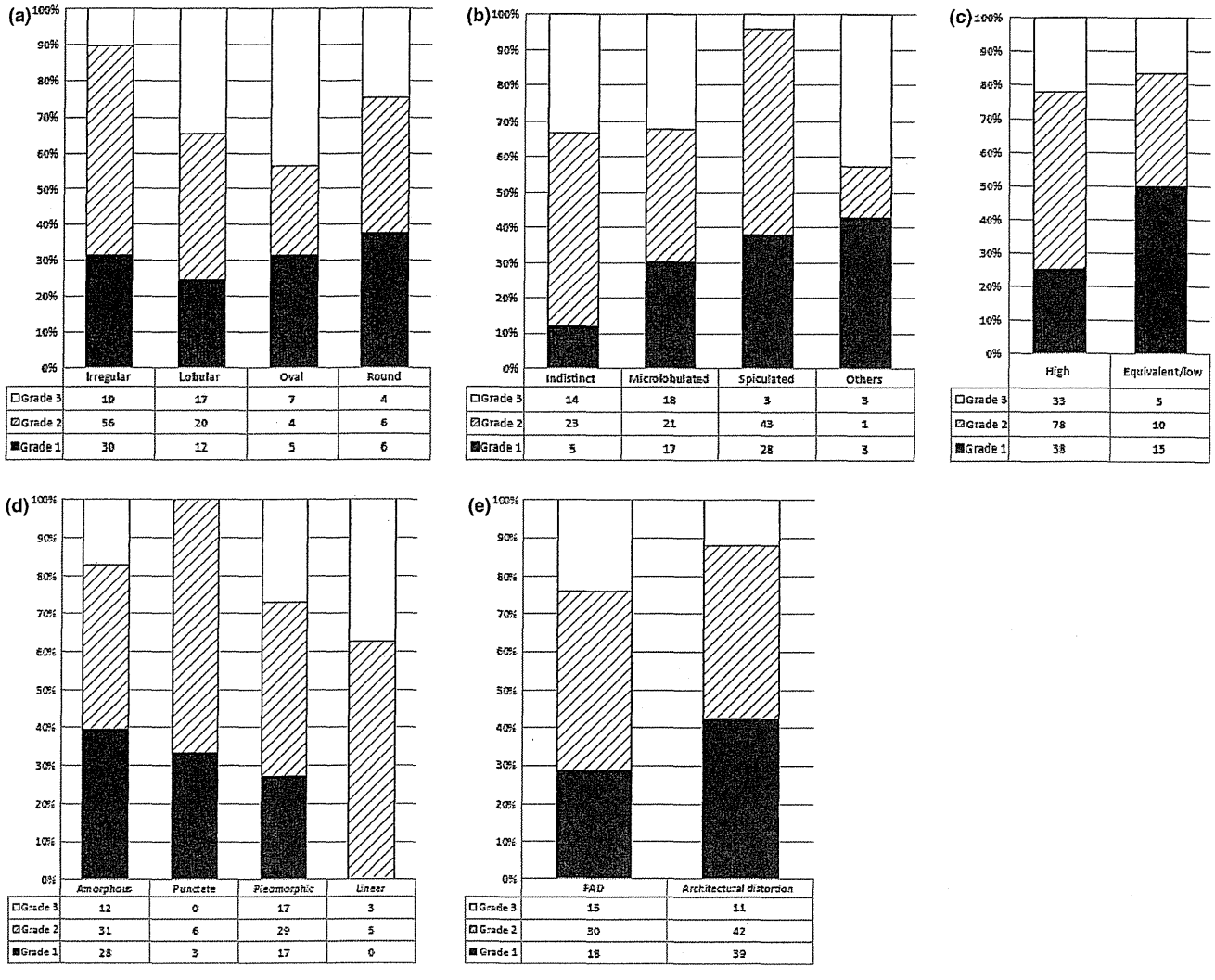

Fig. 3. Correlation between mammographic findings and histological grade: (a) mass shape, (b) margin, (c) density, (d) calcification shape, and (e) focal asymmetric density (FAD) and architectural distortion.

doi: 10.1111/j.1349-7006.2011.02088.x

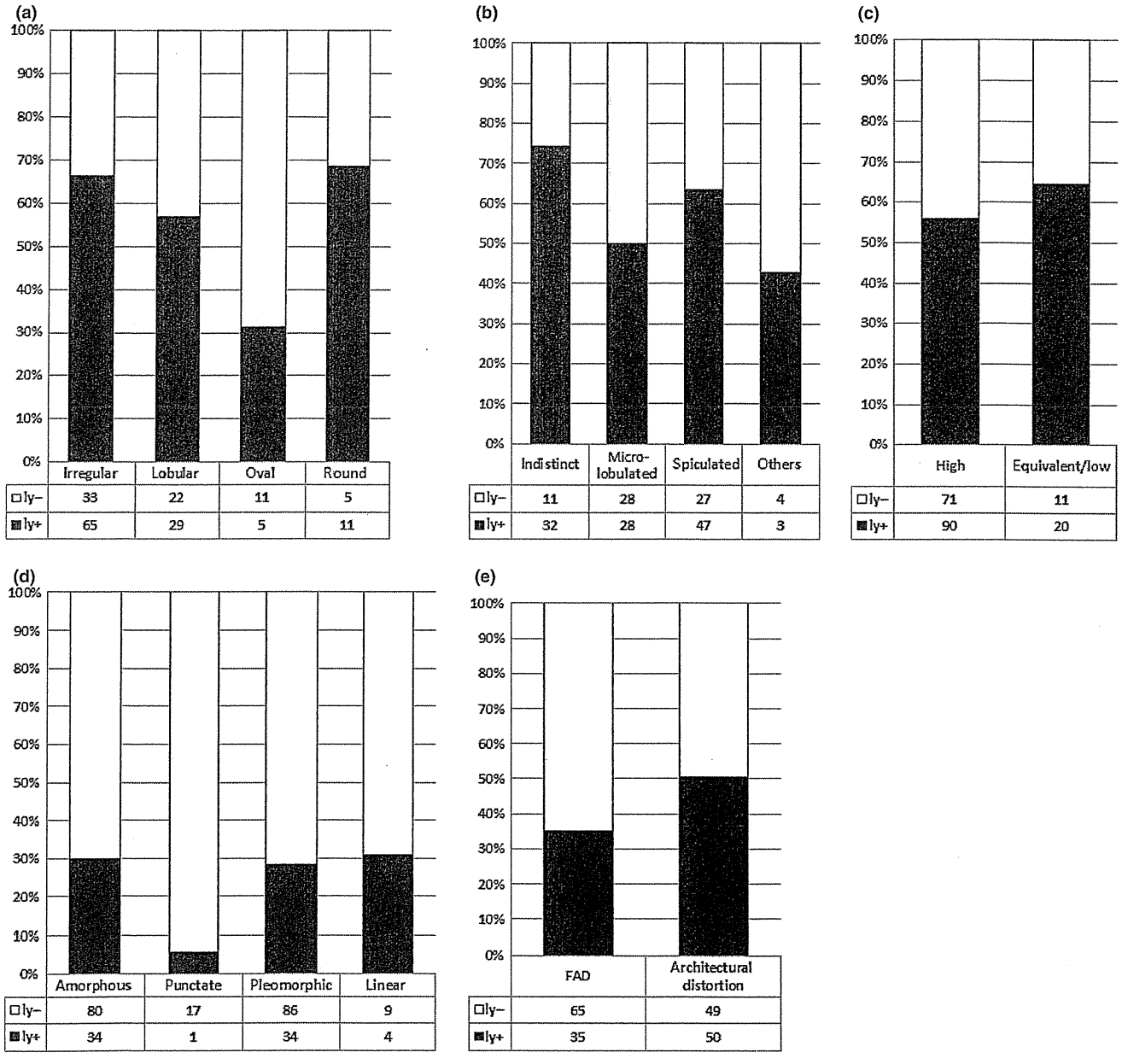

Fig. 4. Correlation between mammographic findings and lymphovascular invasion: (a) mass shape, (b) margin, (c) density, (d) calcification shape, and (e) focal asymmetric density (FAD) and architectural distortion. ly–, no lymphovascular invasion; ly+, lymphovascular invasion.

There were no significant differences according to calcification shape and the presence of architectural distortion.

Discussion

Histological grade is well known to have a strong correlation with clinical outcome in patients with breast cancer.[4] Accumulating clinical evidence suggests that prognostic factors influencing breast cancer extend beyond the traditional tumor histological grade.[17] Several factors, including ER expression, HER2 status, and lymphovascular invasion, have been clearly demonstrated in recent years to contribute significantly to the management and subsequent prognosis of patients with breast cancer.[7,18] Therefore, an accurate correlation between mammographic findings and their corresponding histopathological features is considered most important in mammographic evaluation. Mammographic findings may provide insights into pathological and biological features, including tumor cell characteristics, histological grade, and cell proliferation. We attempted to determine which finding is more relevant with regard to the newly defined subtype of breast carcinoma cells. Therefore, the purpose of the present study was to evaluate the correlation between mammographic findings (e.g. mass shape, margin, density, calcification shape, FAD, and the presence of architectural distortion) with intrinsic subtype, histological grade, lymphovascular invasion, and the Ki-67 labeling index in breast cancer patients.

Several previous studies evaluated the correlation between mammographic findings and histopathological characteristics in individual patients.[8,19–21] A number of independent groups demonstrated that masses with a spiculated periphery were associated with a good outcome in patients.[19,20] Conversely,

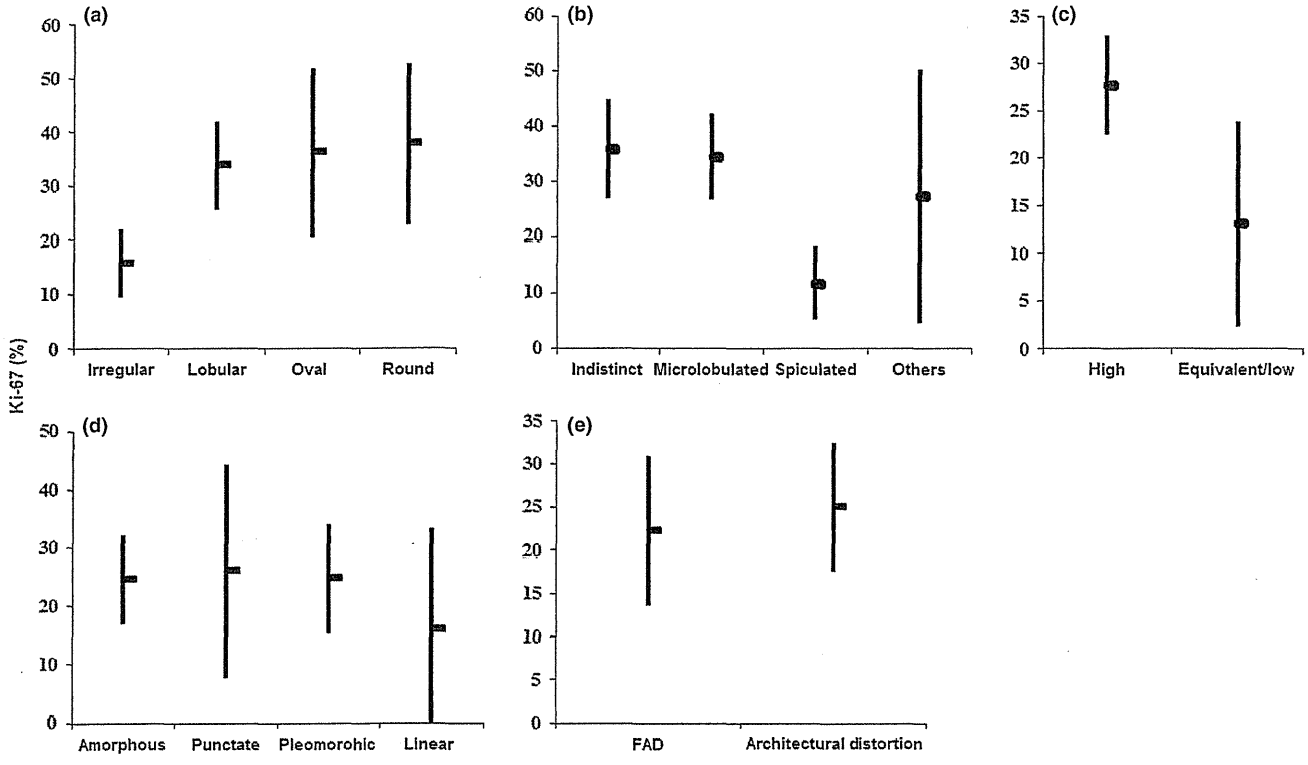

Fig. 5. Correlation between mammographic findings and Ki-67 labeling index: (a) mass shape, (b) margin, (c) density, (d) calcification shape, and (e) focal asymmetric density (FAD) and architectural distortion.

well-defined masses were associated with triple-negative breast cancer.[8,21] The results of the present study demonstrate that is a higher incidence of lower histological grade in masses with an irregular shape and/or spiculated margins, although a higher histological grade is not necessarily associated with irregular mass shape or spiculated margins. In addition, correlation of mammographic findings with the intrinsic subtype demonstrated that irregular mass shape and/or spiculated margin masses were significantly more frequently detected in luminal A breast cancers than in the other subtypes in this cohort of Japanese patients. However, oval and round mass shape and/or indistinct and microlobulated margin masses were significantly more frequently detected in triple-negative breast cancers or HER breast cancers. As for architectural distortion, the ratio of architectural distortion was significantly higher in luminal A cases and also tended to be associated with histological Grade 1. Together, these results suggest that poorly differentiated breast carcinoma cells are associated with good histological grade and luminal A subclassification. However, well-differentiated carcinoma cells are associated with adverse clinical grading and negative ER status.

Previous studies have demonstrated that these differentiations were related somewhat with adhesion factors.[22,23] Loss of adhesion factors in carcinoma cell is considered to play a role in the characteristic histological appearance of invasive carcinoma as loosely dispersed linear columns of cells and a typical discrete mass.[22] This more diffuse infiltrative pattern may explain some of the typical imaging appearances of tumors, such as spiculation and distortion.[22] In addition, adhesion factors are correlated with high histologic grade.[23] Therefore, adhesion factors may be considered to be correlated with the results of the present study in that spiculated breast cancers have a good clinical outcome and histological Grade 1. However, it is also true that numerous biological mechanisms underlying the association between the process of infiltration and histopathological characteristics remain unknown and that further investigations are required to confirm interpretation of mammography in terms of the biological and histopathologic characteristics of tumors.

To the best of our knowledge, this is the first study to compare mammographic findings with the Ki-67 labeling index and histopathological lymphovascular invasion. The results of the present study demonstrated that there was a higher incidence of a lower Ki-67 labeling index in tumors with an irregular mass shape, spiculated periphery, and equivalent or low mass density. Irregular mass shape and a spiculated periphery are well-known predictors of malignancy, but the results of the present study seem to suggest that findings of irregular shape and a spiculated periphery are relatively good prognostic predictors in terms of the Ki-67 labeling index. In addition, the results of the present study demonstrate that lymphovascular invasion was significantly greater in cases in which there was architectural distortion; however, the incidence of lymphovascular invasion was not significantly higher in spiculated masses. These results all suggest that the correlation between findings of radiological dist ortion and the mechanisms of lymphovascular invasion remain unknown and further investigations are required.

We also examined the correlation between mammographic calcification shape and histopathological characteristics. Previous studies have reported that triple-negative breast cancers are more likely to exhibit comedo calcifications.[8] In addition, the high frequency of comedo calcification in triple-negative breast cancers may represent a consequence of high histologic grade.[8] The presence of mammographic comedo calcification has also been reported to be associated with a poor prognosis in small screening-detected invasive cancers.[19] The results of the present study also demonstrate that non-necrotic calcifications, including amorphous and punctate calcification, are associated with a higher ratio of luminal A cases, whereas necrotic calcifications, including pleomorphic and linear calcification, were

doi: 10.1111/j.1349-7006.2011.02088.x

associated with a higher ratio of HER breast cancers. In addition, necrotic calcifications tended to be associated with a higher histological grade than non-necrotic calcifications. Therefore, the results suggest that the type of calcification may become a prognostic factor for breast malignancies.

We noted significant differences in the mammographic features of different primary breast cancer immunophenotypes in the present study. Stratifying the mammographic features according to immunophenotypes reveals distinct differences among cancer subtypes. However, the limitations of the present study include that fact that the study was retrospective in nature and was performed in a single institute, namely Tohoku University Hospital. Therefore, further investigations are needed, including analysis in several different institutions to further refine the new mammographic criteria. Biological and histopathological differences may result in imaging differences that may help us better understand the development of breast cancer. These proposed mammographic diagnostic criteria based on biological characteristics may contribute to a more accurate prediction of the biological behavior of breast malignancies.

Acknowledgments

The authors thank medical technologist Mr Masahiro Sai for his excellent technical assistance for mammography. The authors also thank medical technologist Ms Yayoi Takahashi for excellent technical assistance with the immunohistochemical staining. This work was supported, in part, by a Grant-in Aid from Kurokawa Cancer Research Foundation.

Disclosure Statement

The authors have no conflict of interest.

References

1 Nystrom L, Rutqvist L, Wall S *et al.* Breast cancer screening with mammography; overview of Swedish randomized trials. *Lancet* 1993; **341**: 973–8.
2 Tabar L, Vitak B, Chen HH *et al.* Beyond randomized controlled trials: organized mammographic screening substantially reduces breast carcinoma mortality. *Cancer* 2001; **91**: 1724–31.
3 Carter CL, Allen C, Henson DE. Relation of tumour size, lymph node status, and survival in 24,740 breast cancer cases. *Cancer* 1989; **63**: 181–7.
4 Elston CW, Ellis IO. Pathological prognostic factors in breast cancer. I. The value of histological grade in breast cancer: experience from a large study with long-term follow-up. *Histopathology* 1991; **19**: 403–10.
5 Lee AHS, Pinder SE, Macmillan RD *et al.* Prognostic value of lymph vascular invasion in women with lymph node negative invasive breast carcinoma. *Eur J Cancer* 2006; **42**: 357–62.
6 Bauer KR, Brown M, Cress RD *et al.* Descriptive analysis of estrogen receptor (ER)-negative, progesterone receptor (PR)-negative, and HER2-negative invasive breast cancer, the so-called triple-negative phenotype: a population-based study from the California Cancer Registry. *Cancer* 2007; **109**: 1721–8.
7 Goldhirsch A, Ingle JN, Gelber RD *et al.* Thresholds for therapies: highlights of the St Gallen international expert consensus on the primary therapy of early breast cancer 2009. *Ann Oncol* 2009; **20**: 1319–29.
8 Luck AA, Evans AJ, James JJ *et al.* Breast carcinoma with basal phenotype: mammographic findings. *AJR Am J Roentgenol* 2008; **191**: 346–51.
9 Tamaki K, Sasano H, Ishida T *et al.* Comparison of core needle biopsy (CNB) and surgical specimens for accurate preoperative evaluation of ER, PgR and HER2 status of breast cancer patients. *Cancer Sci* 2010; **101**: 2074–9.
10 D'Orsi CJ, Bassett LW, Berg WA *et al. Breast Imaging Reporting and Data System: ACR BI-RADS-Mammography*, 4th edn. Reston, Virginia: American College of Radiology, 2003.
11 Tavassoli FA, Devilee P. *World Health Organization Classification of Tumors. Tumor of the Breast and Females Gentia Organs*. Lyon: IARC Press, 2003.
12 Rosen PP. *Rosen's Breast Pathology*, 3rd edn. Philadelphia: Lippincott Williams & Wilkins, 2009.
13 Allred DC, Harvey JM, Berardo M, Clark GM. Prognostic and predictive factors in breast cancer by immunohistochemical analysis. *Mod Pathol* 1998; **11**: 155–68.
14 Wolff AC, Hammond MH, Schwartz JN *et al.* American Society of Clinical Oncology/College of American Pathologists guideline recommendations for human epidermal growth factor receptor 2 testing in breast cancer. *J Clin Oncol* 2007; **25**: 118–45.
15 Spyratos F, Ferrero-Pous M, Trassard M *et al.* Correlation between MIB-1 and other proliferation marker clinical implications of the MIB-1 cutoff value. *Cancer* 2002; **94**: 2151–9.
16 Goldhirsch A, Wood WC, Coates AS *et al.* Strategies for subtypes-dealing with the diversity of breast cancer: highlights of the St Gallen International Expert Consensus on the Primary Therapy of Early Breast Cancer 2011. *Ann Oncol* 2011; **22**: 1736–47.
17 Taneja S, Evans AJ, Rakha EA *et al.* The mammographic correlations of a new immunohistochemical classification of invasive breast cancer. *Clin Radiol* 2008; **63**: 1228–35.
18 Jalava P, Kuopio T, Juntti-Patinen L *et al.* Ki67 immunohistochemistry: a valuable marker in prognostication but with a risk of misclassification: proliferation subgroups formed based on Ki67 immunoreactivity and standardized mitotic index. *Histopathology* 2006; **48**: 674–82.
19 Tabar L, Tony Chen HH, Amy Yen MF *et al.* Mammographic tumor features can predict long-term outcomes reliably in women with 1–14-mm invasive breast carcinoma. *Cancer* 2004; **101**: 1745–59.
20 Evan AJ, Pinder SE, James JJ *et al.* Is mammographic spiculation an independent, good prognostic factor in screening detected invasive breast cancer? *AJR Am J Roentgenol* 2006; **187**: 1377–80.
21 Ko ES, Lee BH, Kim HA *et al.* Triple-negative breast cancer: correlation between imaging and pathological findings. *Eur Radiol* 2010; **20**: 1111–7.
22 Doyle S, Evans AJ, Rakha EA *et al.* Influence of E-cadherin expression on the mammographic appearance of invasive nonlobular breat carcinoma detected at screening. *Radiology* 2009; **253**: 51–5.
23 Gastl G, Spizzo G, Obrist P *et al.* Ep-CAM overexpression in breast cancer as a predictor of survival. *Lancet* 2000; **356**: 1981–2.

Cancer Science
The official journal of the Japanese Cancer Association JCA

Multidetector row helical computed tomography for invasive ductal carcinoma of the breast: Correlation between radiological findings and the corresponding biological characteristics of patients

Kentaro Tamaki,[1,2,3,5] Takanori Ishida,[1] Minoru Miyashita,[1] Masakazu Amari,[1] Naoko Mori,[4] Noriaki Ohuchi,[1] Nobumitsu Tamaki[3] and Hironobu Sasano[2]

[1]Department of Surgical Oncology, Tohoku University Graduate School of Medicine, Miyagi; [2]Department of Pathology, Tohoku University Hospital, Miyagi; [3]Department of Breast Surgery, Nahanishi Clinic, Okinawa; [4]Department of Diagnostic Radiology, Tohoku University Graduate School of Medicine, Miyagi, Japan

(Received August 28, 2011/Revised September 30, 2011/Accepted October 4, 2011/Accepted manuscript online October 8, 2011/Article first published online November 3, 2011)

The aim of this study is to evaluate the correlation between multidetector row helical computed tomography (MDCT) findings and the histopathological characteristics of patients with invasive ductal carcinoma. We retrospectively reviewed MDCT findings and the corresponding histopathological features of 442 women with invasive ductal carcinoma. We received informed consent from the patients and the protocol was approved by the Ethics Committee at Tohoku University. The median age was 53 years (26–89 years). We examined the MDCT findings based on mass shape classified into well, moderate, poorly and scattered demarcated shapes, the enhancement pattern classified into homogenous, heterogeneous, rim and poor, and mass density classified into high, intermediate or low. We subsequently compared these radiological findings with the histological characteristics and clinical outcome. Poorly demarcated types were higher in ER+/HER2– ($P = 0.008$), while the well-demarcated type was higher in ER–/HER2– and ER–/HER2+ ($P < 0.001$ and $P = 0.010$). Rim pattern was higher in ER–/HER2– ($P < 0.001$). Intermediate or low density was higher in ER–/HER2– ($P < 0.001$, respectively). Further analysis based on histological grade, mitotic counts and lymphovascular invasion demonstrated that the well-demarcated shape was higher in grade 2 and 3 ($P = 0.006$ and $P < 0.001$, respectively), and rim pattern was observed in grade 3 ($P < 0.001$). Regarding mitotic counts, poorly and scattered demarcated shapes were observed in score 1 ($P = 0.008$ and $P = 0.014$), while well-demarcated shape and rim enhancement were observed in score 3 ($P < 0.001$, respectively). Lymphovascular invasion correlated with a moderate demarcated shape ($P = 0.029$). Regarding recurrence rates, there were statistically significant differences between well and moderate, poorly or scattered demarcated shapes ($P = 0.007$, 0.028 and 0.035, respectively). These proposed MDCT diagnostic criteria based on biological characteristics contribute to more accurately predicting the biological behavior of breast cancer patients. (*Cancer Sci* 2012; 103: 67–72)

Histological tumor type, grade, lymphovascular invasion and molecular markers such as estrogen receptor (ER) and human epidermal growth factor receptor 2 (HER2) status are standard prognostic indicators in breast cancer patients.[1–3] This histological information can contribute to an optimal selection of treatment strategy including endocrine therapy, chemotherapy and targeted therapy in individual patients with breast cancer.[4,5] Several previous studies examined the correlation between radiological findings and the corresponding histopathological characteristics.[6–11] A number of independent studies demonstrated that spiculated periphery masses in mammography were associated with a good outcome, whereas well-defined masses were associated with triple-negative breast cancer cases.[7,8] In addition, a spiculated margin of breast cancer on high spatial resolution dynamic magnetic resonance imaging (MRI) was reported to be able to predict a lower histological grade.[9] As for ultrasonography, a poorly circumscribed margin, abrupt boundary and a hypoechoic or complex echo pattern were reported to be more frequent in grade 3 than in grade 1–2 invasive cancer cases.[10] Therefore, an accurate correlation of radiological findings with their corresponding histopathological features is considered one of the most important in imaging evaluation of breast malignancies, especially with reference to the study of biological features of the patients.

The recent development of multidetector row helical computed tomography (MDCT) has markedly improved the resolution that can be achieved in CT scanning, allowing the entire breast to be scanned in thin slices.[12,13] This instrument can detect much smaller lesions and provide more detailed information regarding the extent of breast cancer infiltration because of faster scanning, a wider area of scan coverage and higher resolution of the volume data than single helical CT.[12,13] However, to the best of our knowledge, no studies have reported on the correlation between these MDCT findings and the corresponding biological characteristics in individual patients with breast cancer. Therefore, in the present study, we evaluated the MDCT findings and compared the histological characteristics including ER, HER2 status, histological grade, mitotic counts of the cancer cells and lymphovascular invasion in a retrospective manner.

Materials and Methods

Patients. We retrospectively reviewed the MDCT findings and histopathological features of 442 invasive ductal carcinoma of the breast for which surgery was performed in Tohoku University Hospital in Sendai Japan from January 2005 to June 2010. We received informed consent from all patients and the protocol for the present study was approved by the Ethics Committee at Tohoku University Graduate School of Medicine. The median age of the patients was 53 years (range 26–89 years). Table 1 summarizes the patient characteristics.

Imaging devices and breast tissue specimens. The MDCT evaluations were performed using a 16-row detector CT system (Somatom Sensation Cardiac; Siemens Medical Solutions,

[5]To whom correspondence should be addressed.
E-mail: nahanisikenta@yahoo.co.jp

doi: 10.1111/j.1349-7006.2011.02116.x

Table 1. Patient characteristics

Patient age, median (range) (years)	53 (26–89)
Hormone receptor and HER2 expression	
ER+/HER2−	327
ER+/HER2+	29
ER−/HER2−	55
ER−/HER2+	31
Histological grade	
HG1	149
HG2	213
HG3	80
Mitotic counts of carcinoma cells	
Score 1	298
Score 2	72
Score 3	72
Lymphovascular invasion	
Ly+	220
Ly−	222

ER, estrogen receptor; HER2, human epidermal growth factor receptor 2; HG, histological grade; Ly, lymphovascular invasion; +, positive; −, negative.

Table 2. Definition of MDCT findings

	Definition
Tumor shape	
Well demarcated	Oval mass shape and circumscribed periphery
Moderate demarcated	Mixed contour of well and poorly demarcated shape
Poorly demarcated	Irregular mass shape and spiculated periphery
Scattered demarcated	Lesion with multiple spotted foci
Enhancement pattern	
Homogenous	Diffuse and monotonous enhancement pattern
Heterogenous	Mosaic pattern
Rim	Enhancement only in periphery of the tumor
Poor	Weak enhancement
Density	
High	High density compared with the normal mammary gland
Intermediate or low	Equal or low density compared with the normal mammary gland

MDCT, multidetector row helical computed tomography.

Erlangen, Germany). A total of 2 mL/kg of nonionic iodine contrast materials (300 mg I/mL) was injected at a rate of 2.0 mL/s. The CT data acquisition started 60 s after commencing the injection of contrast medium. We used an X-ray tube modulation system (CARE Dose 4D; Siemens Medical Solutions). The X-ray tube voltages were 80, 100 or 120 kV and the quality reference tube current-time product was set at 120 mAs. The CT was performed in a craniocaudal direction with a section thickness of 0.75 mm and a table feed of 12 mm per rotation, resulting in a pitch factor of 1. The gantry rotation time was 0.5 s. Transverse CT images were reconstructed using a section thickness and increment of 1 mm each. The additional reconstruction was achieved by targeting the relevant side of the breast with the same thickness and increment. All data were sent to the Advantage Workstation v4.1/4.2 (GE Healthcare, Milwaukee, WI, USA).

The slides of the cases were stained with hematoxylin–eosin (HE) and immunohistochemical antibody for ER and HER2. Surgical specimens had been fixed in 10% formaldehyde solution and cut into serial 5-mm-thick slices, embedded in paraffin, cut into 4-μm-thick sections, and placed on the glue-coated glass slides. We used the avidin–streptavidin immunoperoxidase method using the clone 6F11 antibody (Ventana, Tucson, AZ, USA) in an automated immunostainer (Benchmark System; Ventana). A standardized immunohistochemistry kit (HercepTest for Immunoenzymatic Staining; Dako, Copenhagen, Denmark) was used for HER2 staining.

Imaging and histopathological analyses. Two experienced breast physicians and one experienced radiologist independently evaluated the MDCT findings of all cases examined in the present study. These three investigators were blinded to the histopathological diagnosis and the clinical outcome of the patients. If there were discrepancies between the investigators, they reached a final decision using consensus evaluations from eight experienced breast physicians and radiologists. We recorded tumor shape, enhancement pattern and density. Table 2 summarizes the definition of MDCT findings. Tumor shape was defined on the basis of gross tumor configuration from stellate to circumscribed, and tentatively classified into a well-demarcated shape including an oval mass shape and circumscribed periphery, a poorly demarcated shape including an irregular mass shape and spiculated periphery, a moderate demarcated shape having a mixed contour and a scattered demarcated shape (Fig. 1). The enhancement pattern was tentatively classified into homogenous, heterogenous, rim and poor enhancement (Fig. 1). Density of the lesion after injection of contrast media was subsequently compared with that of normal mammary gland and tentatively classified into high and intermediate or low (Fig. 1).

Two of the experienced pathologists independently evaluated the surgical pathology specimens, respectively. Histopathological evaluation was based on the World Health Organization histological classification of tumors of the breast and *Rosen's Breast Pathology*.[14,15] Estrogen receptor was determined by nuclear staining graded from 0 to 8 using the Allred score, and positive was grade 3 or more.[16] With regard to HER2 evaluation, membranous staining was graded as follows: score 0–1+, 2+ and 3+.[17] Scoring of 2+ cases were added in the other examination of fluorescence *in situ* hybridization (FISH) that was used to calculate the gene copy ratio of HER2-to-CEP17 (PathVysion HER2 DNA Probe kit; Abbott, Chicago, IL, USA). Positive was defined as either HER2 : CEP17 signal ratio (FISH score) >2.2.[17] Histological grades and mitotic counts were assessed according to the criteria of Elston and Ellis.[2] We also identified the presence or absence of lymphovascular invasion according to *Rosen's Breast Pathology*.[15]

We examined the MDCT findings including tumor shape, enhancement pattern and density with the histopathological characteristics including ER, HER2 status, histological grade, mitotic counts and lymphovascular invasion. In addition, we examined the correlation between MDCT findings and clinical outcome including recurrence rate and recurrence-free survival of the patients.

Statistical analysis. To compare the MDCT findings with the histopathological findings, multivariate statistics were used. All analyses were performed with the use of statistical software (SPSS, version 10.0; SPSS, Chicago, IL, USA), with $P < 0.05$ indicating a significant difference.

Results

Comparison of MDCT findings with ER and HER2 status. Table 3 summarizes the results of the numbers and ratios of each MDCT findings according to ER and HER2 status. There were statistically higher cases of moderate and poorly in the

doi: 10.1111/j.1349-7006.2011.02116.x

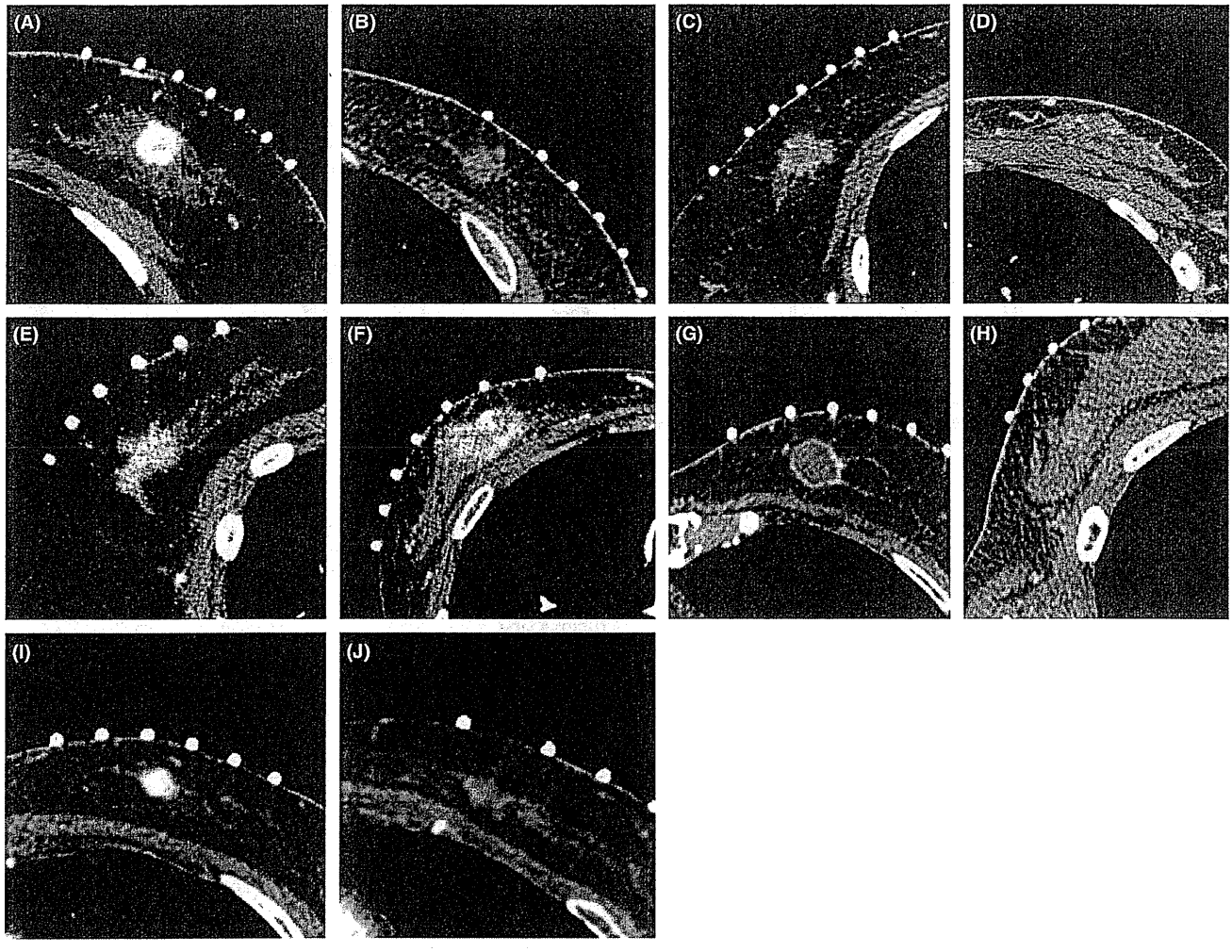

Fig. 1. Representative images of tumor shape, enhancement pattern and density according to multidetector row helical computed tomography findings. (A) Well-demarcated shape, (B) moderate demarcated shape, (C) poorly demarcated shape, (D) scattered demarcated shape, (E) homogenous enhancement pattern, (F) heterogenous pattern, (G) rim pattern, (H) poor enhancement, (I) high density and (J) intermediate or low density.

ER+/HER2− group ($P = 0.014$ and $P = 0.008$, respectively), well in the ER−/HER2− group ($P < 0.001$) and well in the ER−/HER2+ group ($P = 0.010$). However, there were statistically lower ratios of well-demarcated shape compared with other tumor shapes in the ER+/HER2− group ($P < 0.001$) and of poorly in the ER−/HER2− group ($P = 0.004$). Regarding enhancement patterns and density, there were statistically higher cases demonstrating rim pattern and/or intermediate and low density in the ER−/HER2− group ($P < 0.001$, respectively). However, there were statistically lower ratios of rim in the ER+/HER2− group ($P < 0.001$) and of homogenous pattern in the ER−/HER2− group ($P = 0.014$), and of high density in the ER−/HER2− group ($P < 0.001$) (Table 3).

Comparison of MDCT findings with histological grades. Table 4 summarizes the results of the numbers and ratios of each MDCT finding according to histological grade. As for mass shape, there was a statistically higher ratio of well in the grade 3 group ($P < 0.001$) and poorly in the grade 1 group ($P = 0.012$), whereas lower ratios of well in the grade 1 and grade 2 groups ($P < 0.001$ and $P = 0.006$) and moderate and poorly in the grade 3 group ($P = 0.010$ and $P < 0.001$). Regarding the enhancement pattern, there were statistically higher ratios of homogenous in the grade 1 group ($P = 0.041$) and of rim pattern in the grade 3 group ($P < 0.001$). However, there was a statistically lower ratio of homogenous in the grade 3 group ($P = 0.020$) and of rim pattern in the grade 1 group ($P < 0.001$). There was no statistical significance in the correlation between histological grade and density (Table 4).

Comparison of MDCT findings with mitotic counts. Table 5 summarizes the results of the numbers and ratios of each MDCT finding according to mitotic counts. There were statistically higher ratios of poorly in the score 1 group ($P = 0.008$), well in the score 3 group ($P < 0.001$) and scattered in the score 1 group ($P = 0.014$), whereas lower ratios of well-demarcated shape in the score 1 group ($P = 0.015$) and poorly demarcated shape in the score 3 group ($P = 0.007$). As for the enhancement pattern, there were higher ratios of rim pattern in the score 2 and score 3 groups ($P = 0.004$ and $P < 0.001$, respectively) and poor pattern in the score 1 group ($P = 0.027$), whereas a lower ratio of rim pattern in the score 1 group ($P < 0.001$). There was no statistical significance in the correlation between mitotic counts and density (Table 5).

Comparison of MDCT findings with lymphovascular invasion. Table 6 summarizes the results of the numbers and ratios of each MDCT finding according to lymphovascular invasion. There was a statistically higher ratio of lymphovascular

Table 3. Comparison of MDCT findings with ER and HER2 status

	ER+/HER2−	ER+/HER2+	ER−/HER2−	ER−/HER2+
Tumor shape				
Well	23	5	24*	9*
Moderate	169*	12	20	13
Poorly	110*	8	8	8
Scattered	25	4	5	1
Enhancement pattern				
Homogenous	142	10	14	14
Heterogenous	162	16	26	15
Rim	8	2	12*	2
Poor	15	1	3	0
Density				
High	198	21	20	22
Intermediate/low	129	8	35*	9

*Higher ratio $P < 0.05$. ER, estrogen receptor; HER2, human epidermal growth factor receptor 2; MDCT, multidetector row helical computed tomography; +, positive; −, negative.

Table 4. Comparison of MDCT findings with histological grade

	Grade 1	Grade 2	Grade 3
Tumor shape			
Well	3	19	38*
Moderate	75	109	28
Poorly	61*	72	13
Scattered	10	13	1
Enhancement pattern			
Homogenous	72*	88	24
Heterogenous	76	103	35
Rim	1	13	19*
Poor	0	9	2
Density			
High	92	127	48
Intermediate/low	57	86	32

*Higher ratio $P < 0.05$. MDCT, multidetector row helical computed tomography.

Table 5. Comparison of MDCT findings with mitotic counts

	Score 1	Score 2	Score 3
Tumor shape			
Well	27	15	28*
Moderate	142	33	31
Poorly	103*	22	9
Scattered	28*	2	2
Enhancement pattern			
Homogenous	127	26	21
Heterogenous	147	31	31
Rim	4	14*	16*
Poor	22*	1	2
Density			
High	183	46	38
Intermediate/low	115	26	34

*Higher ratio $P < 0.05$. MDCT, multidetector row helical computed tomography.

Table 6. Comparison of MDCT findings with lymphovascular invasion

	Ly+	Ly−
Tumor shape		
Well	36	26
Moderate	113*	91
Poorly	62	72
Scattered	9	33
Enhancement pattern		
Homogenous	82	92
Heterogenous	110	99
Rim	19	11
Poor	9	20
Density		
High	139	128
Intermediate/low	81	94

*Higher ratio $P < 0.05$. Ly, lymphovascular invasion; MDCT, multidetector row helical computed tomography; +, positive; −, negative.

invasion in the moderate demarcated shape group ($P = 0.029$). However, there were statistically lower ratios of lymphovascular invasion in the scattered and/or poor enhancement pattern ($P < 0.001$ and $P = 0.037$) (Table 6).

Comparison of MDCT findings with clinical outcome of the patients. Disease recurrence rates according to tumor shape were 25.0% in the well-demarcated shape, 6.7% in the moderate demarcated shape, 8.8% in the poorly demarcated shape and 0% in the scattered demarcated shape. There were statistically significant differences between well and moderate, poorly or scattered demarcated shapes ($P = 0.007$, 0.028 and 0.035, respectively). Recurrence rates according to enhancement pattern were 5.7% in homogenous, 10.6% in heterogenous, 20.0% in rim and 9.1% in the rim enhancement pattern. There were no statistically significant differences according to enhancement patterns. Recurrence rates according to density were 9.0% in high and 8.9% in intermediate or low density and there were no statistically significant differences between these two groups. Figure 2 shows the recurrence-free survival in relation to tumor shape and enhancement patterns according to the Kaplan–Meier method. There were statistically significant differences between the well-demarcated shape and the moderate or scattered demarcated shape ($P = 0.024$ and 0.038, respectively).

Discussion

Breast cancer is a disease associated with heterogeneous outcomes and numerous studies have been reported regarding the establishment of prognostic factors of individual patients. Traditional prognostic factors that were correlated with the overall survival of patients include histological grade, mitotic counts and lymphovascular invasion of individual cases.[2,18] Several molecular prognostic factors including ER and HER2 status have over the past few years been clearly demonstrated to contribute significantly to the management and subsequent prognosis of patients with breast cancer.[18,19] Therefore, an accurate correlation of radiological findings with their corresponding histopathological features is considered most important in the radiological evaluation of patients with breast cancer. In addition, the recognition of how many radiological features obtained might actually reflect the prognosis of individual patients is considered markedly important in gaining insight into how the tumor proliferates and into potentially determining which tumors can be managed with aggressive adjuvant treatment. The purpose of the present study is therefore to evaluate the correlation of MDCT findings including tumor shape, enhancement pattern and density with ER expression, HER2 status, histological grade, mitotic counts and lymphovascular invasion in Japanese patients with breast cancer.

doi: 10.1111/j.1349-7006.2011.02116.x

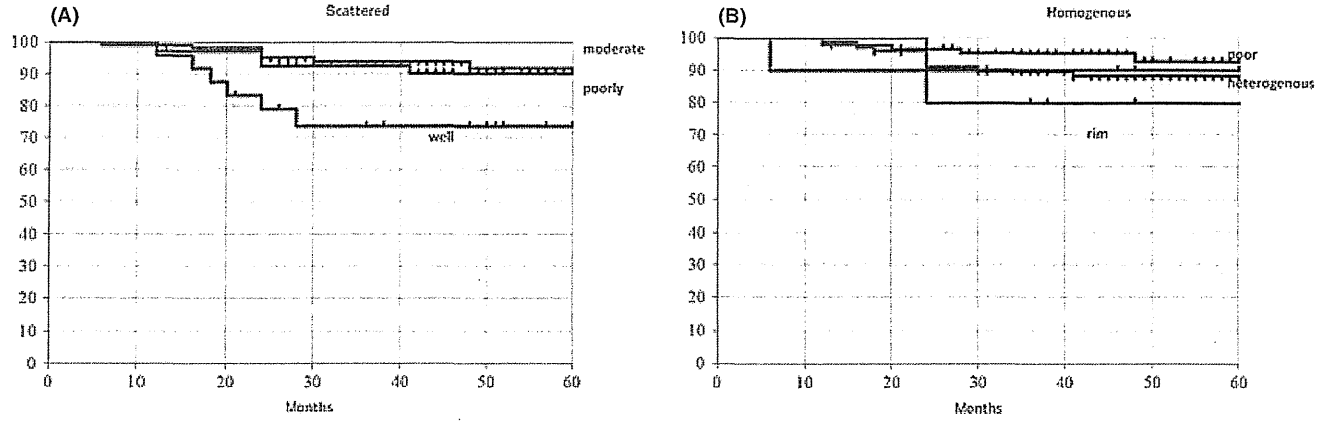

Fig. 2. Recurrence-free survival according to multidetector row helical computed tomography findings using the Kaplan–Meier method. (A) Tumor shape and (B) enhancement pattern.

Several previous studies evaluated the correlation between radiological findings including mammography, ultrasonography and MRI and histopathological characteristics of individual patients.[7–11,20] For mammography, a number of independent study groups demonstrated that spiculated periphery masses were significantly associated with a good outcome for patients,[7,8] but well-defined masses were associated with triple-negative breast cancer.[7,8] Previous studies also compared the ultrasonographic findings of ER-negative/HER2-negative cancers with those of ER-negative/HER2-positive cancers and concluded that ER-negative/HER2-positive breast cancers were likely to demonstrate spiculated margins and to be associated with calcifications.[10] In addition, ER-negative/HER2-negative breast cancers were more likely to show as smooth or circumscribed masses.[10] A spiculated margin in MRI findings did demonstrate an association with positive ER expression and negative HER2 status, and high-grade malignant breast cancers circumscribed margins.[9,20]

Results of the present study did demonstrate that there was a higher incidence of increased ratios of ER+/HER2− type, lower histological grade, lower mitotic counts and a lower ratio of lymphovascular invasion in poorly demarcated masses, whereas the presence of higher ratios of triple-negative type, higher histological grade, higher mitotic counts and lymphovascular invasion were all demonstrated to be associated with well-demarcated masses in the present study. In addition, these results all suggest that poorly demarcated breast cancer was associated with a good clinical outcome, and well-demarcated shape of carcinoma cells was associated with an adverse clinical outcome and negative ER status in carcinoma cells. Results of the present study were similar to those of previously reported studies regarding the correlation between mammography or MRI findings and intrinsic subtype or histological grade of cases.[7–11,20] Inoue *et al.*[21] reported the correlation between MDCT findings and the ratio of malignant cases but they did not necessarily focus on the histopathological characteristics of the cases examined. Therefore, to the best of our knowledge, this is the first study to examine the correlation between MDCT findings and the corresponding histopathological features. However, the mechanisms of the correlation between intrinsic subtype or histological grade and the growth pattern of carcinoma cells have not been elucidated. Therefore, further studies are required to investigate the potential mechanisms of correlation between biological characteristics and the growth pattern of carcinoma cells.

Results of the present study also demonstrated that there were statistically significant correlations of rim enhancement patterns with triple-negative breast cancer and higher histological grade. Rim enhancement was one of the important morphological signs in predicting the worse clinical outcomes. These results all suggest that high angiogenesis might be present in the peripheral lesion of the masses and central necrosis and fibrosis. A previous MRI study also demonstrated the correlation between rim enhancement and large tumor size, higher histological grade or negative hormone receptor status of cases.[22] However, this is the first study examining the correlation between rim enhancement in MDCT findings and biological characteristics of breast malignancies. In general, rim enhancement is more frequently noted in rapidly growing breast carcinomas.

In addition, we also examined the recurrence ratio and recurrence-free survival of patients according to MDCT findings. Results of the present study demonstrated that a well-demarcated shape was associated with a significantly higher recurrence ratio than other groups ($P = 0.007$, 0.028 and 0.035, respectively). A similar tendency was also detected in the rim enhancement pattern but the difference did not reach statistical significance. Therefore, MDCT findings of well-demarcated shape and rim enhancement pattern can become one of the predictors of a worse clinical outcome for patients.

We noted significant differences in the MDCT features of different primary breast cancer types in the present study. Stratifying the MDCT features according to phenotypes reveals distinct differences among cancer subtypes. However, the present study was retrospective and examined in a single institute. Therefore, it is probable that further investigation of not only Japanese women but also other Asian women will confirm the new MDCT criteria. Biological and histopathological differences may result in the imaging differences that might help us better understand breast cancer development. These proposed MDCT diagnostic criteria based on biological characteristics might provide a more accurate prediction of biological behavior of breast malignancies when radiologists evaluate the findings of MDCT.

Acknowledgments

The authors thank Medical Technician Yayoi Takahashi, for her excellent technical assistance for immunohistochemical staining. This work was supported in part by a Grant-in-Aid from Kurokawa Cancer Research Foundation.

Disclosure Statement

The authors have no conflict of interest.

References

1 Carter CL, Allen C, Henson DE *et al.* Relation of tumour size, lymph node status, and survival in 24,740 breast cancer cases. *Cancer* 1989; **63**: 181–7.
2 Elston CW, Ellis IO. Pathological prognostic factors in breast cancer. I. The value of histopathological grade in breast cancer: experience from a large study with long-term follow-up. *Histopathology* 1991; **19**: 403–10.
3 Lee AHS, Pinder SE, Macmillan RD *et al.* Prognostic value of lymph vascular invasion in women with lymph node negative invasive breast carcinoma. *Eur J Cancer* 2006; **42**: 357–62.
4 Bauer KR, Brown M, Cress RD *et al.* Descriptive analysis of estrogen receptor (ER)-negative, progesterone receptor (PR)-negative, and HER2-negative invasive breast cancer, the so-called triple-negative phenotype: a population-based study from the California cancer Registry. *Cancer* 2007; **109**: 1721–8.
5 Tamaki K, Sasano H, Ishida T *et al.* Comparison of core needle biopsy (CNB) and surgical specimens for accurate preoperative evaluation of ER, PgR and HER2 status of breast cancer patients. *Cancer Sci* 2010; **101**: 2074–9.
6 Tamaki K, Sasano H, Ishida T *et al.* The correlation between ultrasonographic findings and pathologic features in breast disorders. *Jpn J Clin Oncol* 2010; **40**: 905–12.
7 Luck AA, Evans AJ, James JJ *et al.* Breast carcinoma with basal phenotype: mammographic findings. *AJR Am J Roentgenol* 2008; **191**: 346–51.
8 Evans AJ, Pinder SE, James JJ *et al.* Is mammographic spiculation an independent, good prognostic factor in screening detected invasive breast cancer? *AJR Am J Roentgenol* 2006; **187**: 1377–80.
9 Lee SH, Cho N, Kim SJ *et al.* Correlation between high resolution dynamic MR features and prognostic factors in breast cancer. *Korean J Radiol* 2008; **9**: 10–8.
10 Kim SH, Seo BK, Lee J *et al.* Correlation of ultrasound findings with histology, tumor grade, and biological markers in breast cancer. *Acta Oncol* 2008; **47**: 1531–8.
11 Amano G, Ohuchi N, Ishibashi T *et al.* Correlation of three-dimensional magnetic resonance imaging with precise histopathological map concerning carcinoma extension in the breast. *Breast Cancer Res Treat* 2000; **60**: 43–55.
12 Takase K, Furuta A, Harada N *et al.* Assessing the extent of breast cancer using multidetector row helical computed tomography. *J Comput Assist Tomogr* 2006; **30**: 479–85.
13 Harada-Shoji N, Yamada T, Ishida T *et al.* Usefulness of lesion image mapping with multidetector-row helical computed tomography using a dedicated skin marker in breast-conserving surgery. *Eur Radiol* 2009; **19**: 868–74.
14 Tavassoli FA, Devilee P. *World Health Organization Classification of Tumors. Tumor of the Breast and Females Gental Organs*. Lyon: IARC Press, 2003.
15 Rosen PP. *Rosen's Breast Pathology*, 3rd edn. Philadelphia, PA, USA: Lippncott Williams & Wilkins, 2009.
16 Allred DC, Harvey JM, Berardo M, Clark GM. Prognostic and predictive factors in breast cancer by immunohistochemical analysis. *Mod Pathol* 1998; **11**: 155–68.
17 Wolff AC, Hammond MH, Schwartz JN *et al.* American Society of Clinical Oncology/College of American Pathologists guideline recommendations for human epidermal growth factor receptor 2 testing in breast cancer. *J Clin Oncol* 2007; **25**: 118–45.
18 Goldhirsch A, Ingle JN, Gelber RD *et al.* Thresholds for therapies: highlights of the St Gallen International Expert Consensus on the primary therapy of early breast cancer 2009. *Ann Oncol* 2009; **20**: 1319–29.
19 Jalava P, Kuopio T, Juntti-Patinen L *et al.* Ki67 immunohistochemistry: a valuable marker in prognostication but with a risk of misclassification: proliferation subgroups formed based on Ki67 immunoreactivity and standardized mitotic index. *Histopathology* 2006; **48**: 674–82.
20 Uematsu T, Kasami M, Yuen S. Triple-negative breast cancer: correlation between MR imaging and pathologic findings. *Radiology* 2009; **250**: 638–47.
21 Inoue M, Sano T, Watai R *et al.* Dynamic multidetector CT of breast tumors: diagnostic features and comparison with conventional techniques. *AJR Am J Roentgenol* 2003; **181**: 679–86.
22 Jeh SK, Kim SH, Kim HS *et al.* Correlation of the apparent diffusion coefficient value and dynamic magnetic resonance imaging findings with prognostic factors in invasive ductal carcinoma. *J Magn Reson Imaging* 2011; **33**: 102–9.

doi: 10.1111/j.1349-7006.2011.02116.x

Cancer Science
The official journal of the Japanese Cancer Association JCA

Nucleobindin 2 in human breast carcinoma as a potent prognostic factor

Shiho Suzuki,[1] Kiyoshi Takagi,[1,5] Yasuhiro Miki,[2] Yoshiaki Onodera,[2] Jun-ichi Akahira,[2] Akiko Ebata,[2,3] Takanori Ishida,[3] Mika Watanabe,[4] Hironobu Sasano[2,4] and Takashi Suzuki[1]

Departments of [1]Pathology and Histotechnology, [2]Anatomic Pathology, [3]Surgical Oncology, Tohoku University Graduate School of Medicine, Sendai; [4]Department of Pathology, Tohoku University Hospital, Sendai, Japan

(Received June 20, 2011/Revised September 15, 2011/Accepted September 27, 2011/Accepted manuscript online October 11, 2011/Article first published online November 17, 2011)

It is well-known that estrogens immensely contribute to the progression of human breast carcinoma, but their detailed molecular mechanisms remain largely unclear. In this study, we identified nucleobindin 2 (*NUCB2*) as a gene associated with recurrence based on microarray data of estrogen receptor (ER)-positive breast carcinoma cases ($n = 10$), and subsequent *in vitro* study showed that *NUCB2* expression was upregulated by estradiol in ER-positive MCF-7 cells. However, *NUCB2* has not yet been examined in breast carcinoma, and its significance remains unknown. Therefore, we further examined the biological functions of *NUCB2* in breast carcinoma using immunohistochemistry and *in vitro* studies. *NUCB2* immunoreactivity was detected in carcinoma cells in 77 of 161 (48%) breast cancer cases, and positively associated with lymph node metastasis and ER status of the patients. In addition, *NUCB2* status was significantly associated with an increased risk of recurrence and adverse clinical outcome of the patients using both univariate and multivariate analyses. Results of siRNA transfection experiments showed that *NUCB2* significantly increased cell proliferation, and migration and invasion properties in both MCF-7 and ER-negative SK-BR-3 cells. These results suggest that *NUCB2* is upregulated by estrogens and plays an important role, especially in the process of metastasis, in breast carcinomas. *NUCB2* status is considered a potent prognostic factor in human breast cancer. (*Cancer Sci* 2012; 103: 136–143)

Breast cancer is one of the most common malignancies in women. Estrogens play an important role in the progression of breast cancer through an interaction with ER, and ER is positive in approximately two-thirds of breast carcinoma cases. The great majority of ER-positive breast carcinomas respond to endocrine therapy such as tamoxifen and aromatase inhibitors, but it is also true that some of these carcinomas acquire clinical resistance to endocrine therapy.[1,2]

Estrogen receptor activates the transcription of various target genes in a ligand-dependent manner by binding EREs located in the promoter region. Various estrogenic functions are characterized by the expression patterns of these genes, which make it extremely important to examine the expression and roles of estrogen-responsive genes to obtain a better understanding of estrogenic actions such as progression, recurrence, and resistance to endocrine therapy.[3] Various estrogen-responsive genes have been identified in breast carcinoma,[4,5] but their detailed clinical significance and/or function remain unclear in a great majority of these genes. Therefore, in this study, we first studied the expression profiles of genes containing ERE in ER-positive breast carcinoma tissues based on microarray data, and identified *NUCB2* as a possible gene associated with recurrence in these patients.

Nucleobindin 2 has a characteristic constitution of functional domains, such as a signal peptide, a Leu/Ile rich region, two Ca^{2+} binding EF-hand domains separated by an acidic amino acid-rich region, and a leucine zipper,[6,7] and has a wide variety of basic cellular functions.[8–10] However, to the best of our knowledge, *NUCB2* has not yet been studied in breast carcinoma. Therefore, we examined *NUCB2* in breast carcinoma using immunohistochemistry and *in vitro* studies to explore its clinical and biological significance.

Materials and Methods

Patients and tissues. Two sets of tissue specimens were evaluated in this study. As a first set, 10 specimens of ER-positive breast carcinoma were obtained from women (age range, 48–74 years) who underwent surgical treatment in 2001 or 2002 in the Department of Surgery, Tohoku University Hospital (Sendai, Japan). All patients received tamoxifen therapy after surgery. The status of recurrence was evaluated whether the first locoregional recurrence or distant metastasis was detected within the follow-up time after surgery (mean, 80 months; range, 37–204 months) or not. These specimens were stored at −80°C for microarray analysis.

As a second set, 161 specimens of invasive ductal carcinoma of human breast were obtained from women who underwent surgical treatment between 1984 and 1997 in the Department of Surgery, Tohoku University Hospital. The patients did not receive chemotherapy, irradiation, or hormonal therapy before the surgery. Review of the charts revealed that 125 patients received adjuvant chemotherapy, 66 patients received tamoxifen therapy, and 12 patients received radiation therapy following surgery. The clinical outcome of the patients was evaluated by disease-free and breast cancer-specific survival. The mean age was 54 years (range, 22–81 years), and the mean follow-up time was 103 months (range, 3–157 months). Mitotic score and histological grade were evaluated according to a previous report.[11] All the specimens were fixed in 10% formalin and embedded in paraffin wax.

Research protocols for this study were approved by the Ethics Committee at Tohoku University School of Medicine (Sendai, Japan).

Laser capture microdissection/microarray analysis. Gene expression profiles of breast carcinoma cells in the first set ($n = 10$) were examined using microarray analysis. Gene expression profile data was assembled previously.[12,13] Briefly, approximately 5000 breast carcinoma cells were laser transferred from the frozen section, and total RNA was subsequently extracted. In this study, we focused on the expression of 519 genes identified to have a functional ERE by Bourdeau *et al.*[14]

Immunohistochemistry. Rabbit polyclonal antibody for *NUCB2* and *HER2* (A0485) were purchased from Aviva Systems Biology (San Diego, CA, USA) and Dako (Carpinteria, CA, USA), respectively. Monoclonal antibodies for ER (ER1D5), PR (MAB429), and Ki-67 (MIB1) were purchased

[5]To whom correspondence should be addressed.
E-mail: k-takagi@med.tohoku.ac.jp

doi: 10.1111/j.1349-7006.2011.02119.x

from Immunotech (Marseille, France), Chemicon (Temecula, CA, USA), and Dako, respectively.

A Histofine Kit (Nichirei, Tokyo, Japan), which incorporates the streptavidin–biotin amplification method, was used. The antigen–antibody complex was visualized with 3,3′-diaminobenzidine and counterstained with hematoxylin. Human tissue of the stomach was used as a positive control for NUCB2 antibody,[15] and normal rabbit IgG was used instead of the primary antibody, as a negative control of NUCB2 immunostaining.

NUCB2 immunoreactivity was detected in the cytoplasm of breast carcinoma cells, and the cases that had more than 10% of positive carcinoma cells were considered positive for NUCB2 status. Immunoreactivity for ER, PR, and Ki-67 was detected in the nucleus, and the immunoreactivity was evaluated in more than 1000 carcinoma cells for each case. The percentage of immunoreactivity, that is, the LI, was determined. Cases with an ER LI or PR LI of more than 10% were considered ER- or PR-positive breast carcinoma, respectively, according to a previous report.[16]

Immunoblotting. The protein of MCF-7 cells was extracted using M-PER Mammalian Protein Extraction Reagent (Pierce Biotechnology, Rockford, IL, USA) with Halt Protease Inhibitor Cocktail (Pierce Biotechnology). Twenty micrograms of the protein (whole cell extracts) was subjected to SDS-PAGE (10% acrylamide gel). Following SDS-PAGE, proteins were transferred onto Hybond-P PVDF membrane (GE Healthcare, Chalfont St Giles, UK). Primary antibody was the same anti-NUCB2 antibody used in the immunohistochemistry (Aviva Systems Biology). Antibody–protein complexes on the blots were detected using ECL Plus Western blotting detection reagents (GE Healthcare), and the protein bands were visualized with a LAS-1000 image analyzer (Fuji Photo Film, Tokyo, Japan).

Real-time PCR. Total RNA was extracted using TRIzol reagent (Invitrogen, Carlsbad, CA, USA), and cDNA was synthesized using a QuantiTect reverse transcription Kit (Qiagen, Hilden, Germany). Real-time PCR was carried out using the LightCycler System and FastStart DNA Master SYBR Green I (Roche Diagnostics, Mannheim, Germany). The primer sequences of NUCB2 and the ribosomal protein L13A (RPL13A) were: NUCB2, 5′-AAAGAAGAGCTACAACGTCA-3′ (forward) and 5′-GTGGCTCAAACTTCAATTC-3′ (reverse); and RPL13A, 5′-CCTGGAGGAGAAGAGGAAAGAGA-3′ (forward) and 5′-TTGAGGACCTCTGTGTATTTGTCAA-3′ (reverse). The NUCB2 mRNA level was calculated as the ratio of the RPL13A mRNA level.

Small interfering RNA transfection. Small interfering RNA for NUCB2 was purchased from Ambion (Austin, TX, USA). The target sequences of siRNA against *NUCB2* were as follows: si1, 5′-UAUCUUCGCACUUUCCACAGGGUGA-3′ (sense) and 5′-UCACCCUGUGGAAAGUGCGAAGAUA-3′ (anti-sense); and si2, 5′-UUGAUUAGCAUAUCUAAAUCUGUGG-3′ (sense) and 5′-CCACAGAUUUAGAUAUGCUAAUCAA-3′ (anti-sense). In addition, medium GC duplex #2 (Invitrogen) was also used as a negative control (siC). The siRNA was transfected using HiperFect transfection reagent (Qiagen).

Cell proliferation, migration, and invasion assays. MCF-7 and SK-BR-3 cells were transfected with NUCB2-specific siRNA or control siRNA in a 96-well culture plate. Three days after transfection, the cell number was evaluated using a Cell Counting Kit-8 (Dojindo, Kumamoto, Japan).

The cell migration assay was carried out using a 24-well plate and Chemotaxicell (8 μm pore size; Kurabo, Osaka, Japan) according to a previous report.[17] MCF-7 and SK-BR-3 cells were plated at the upper chamber, and the cells on the upper surface of the membrane were removed after incubation for 72 h. The migration ability was evaluated as an average number of cells in five middle power fields (×200) randomly selected on the lower surface of the membrane.

The cell invasion assay was carried out using a modified migration assay. The upper surface of the membrane of a Chemotaxicell was coated with 80 mg/cm^2 of Matrigel basement membrane matrix (BD Biosciences, Heidelberg, Germany), and the invasion ability was evaluated as the total number of cells on the lower surface of the membrane.

Results

Comparison of gene expression profiles between recurrent and non-recurrent groups of breast carcinoma patients. The microarray data used in this study are available through the National Center for Biotechnology Information Gene Expression Omnibus database (accession GSE11965, http://www.ncbi.nlm.nih.gov/geo). In this analysis, when the expression ratio of a gene in the recurrence group compared to that in the non-recurrence group was more than 2.0 or <0.5, we determined that the gene was predominantly expressed in the recurrence or non-recurrence group, respectively.

As shown in Figure 1(A), of the 519 genes examined, the number of genes predominantly expressed in the recurrence group (group A) was 17 (3%); the number of genes predominantly expressed in the non-recurrence group (group B) was 35 (7%). A great majority of the genes (467 genes; 90%) had a similar expression level in each of the two groups (ratio 0.5–2.0) (group C). The lists of genes classified in group A and group B are summarized in the right panel of Figure 1(A), and in Table S1. When we carried out gene ontology enrichment analysis between groups A and B (http://cbl-gorilla.cs.technion.ac.il/), no significant enriched gene ontology term was detected. Among the genes in Group A, *NUCB2* showed the highest ratio (4.9) and expression level, indicating its possible involvement in the recurrence in ER-positive breast carcinoma patients after surgery.

The *NUCB2* gene contains functional ERE in the promoter region[14] but the regulation of *NUCB2* expression by estradiol has not been investigated in breast carcinoma cells. As shown in Figure 1(B), NUCB2 mRNA expression was significantly increased by estradiol treatment for 3 days in MCF-7 cells. However, the NUCB2 mRNA expression level was significantly lower ($P < 0.05$, and 0.3-fold) than the basal level, when the cells were treated together with estradiol (10 nM) and a potent ER antagonist ICI 182780 (1 μM). When MCF-7 cells were treated with estradiol (10 nM) and anti-estrogen tamoxifen (10 μM), the NUCB2 mRNA level was not significantly changed compared to the basal level ($P = 0.10$, and 1.5-fold). Estradiol (10 nM) time-dependently induced NUCB2 mRNA expression in MCF-7 cells (Fig. 1C).

***NUCB2* immunolocalization in human breast carcinoma.** As shown in Figure 2(A), immunoblot analysis for *NUCB2* revealed a specific band (approximately 43 kDa) in MCF-7 cells, which confirmed the specificity of the anti-*NUCB2* antibody used in this study.[18] In the immunohistochemistry, *NUCB2* immunoreactivity was detected in the cytoplasm of breast carcinoma cells (Fig. 2B). *NUCB2* immunoreactivity was weakly and focally detected in the epithelial cells of morphologically normal glands (Fig. 2C), but it was negative in the stroma. In the positive control, *NUCB2* was mainly positive in the epithelium of the fundic glands in the stomach (Fig. 2D), as reported previously,[15] whereas no significant immunoreactivity was detected in the same areas of the negative control section (Fig. 2E).

Associations between *NUCB2* immunohistochemical status and various clinicopathological parameters in breast carcinomas are summarized in Table 1. Of 161 cases of breast carcinoma examined in this study, 77 (48%) were *NUCB2*-positive. *NUCB2* status was significantly associated with lymph node metastasis ($P = 0.004$) and ER status ($P = 0.002$) of the patients, whereas no significant association was detected in patients' age, menopausal status, clinical stage, tumor size,

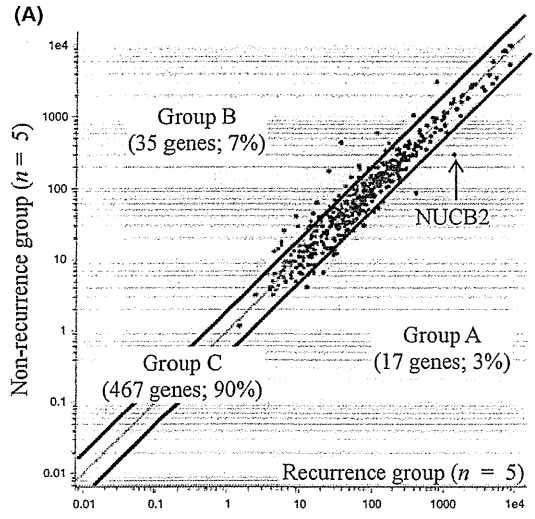

Genes classified as Group A		
Fold†	Common name	Gene symbol
4.9	**NM_005013**	**NUCB2**
4.8	AI824012	NRIP1
3.2	NM_001557	CXCR2
3.0	X02189	ADA
2.6	NM_001874	CPM
2.5	NM_001228	CASP8
2.4	AK023540	BUB1
2.3	NM_016083	CNR1
2.3	AF109161	CITED2
2.3	NM_016580	PCDH12
2.2	NM_001256	CDC27
2.2	BC005312	HLA-DRB4
2.2	AF149096	TGFA
2.1	NM_006889	CD86
2.1	X63575	ATP2B2
2.1	X81006	TRIM31
2.1	AW157548	IGFBP5

†: Expression ratio in the recurrence group to that in the non-recurrence group.

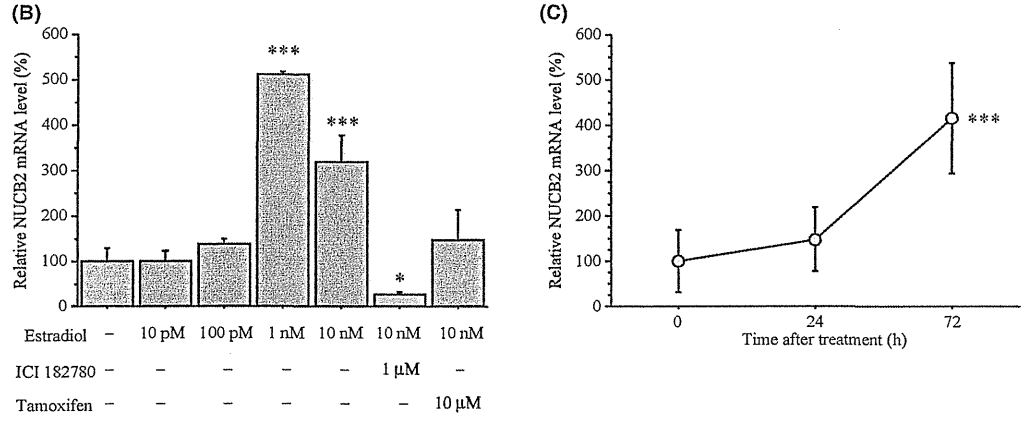

Fig. 1. Nucleobindin 2 (*NUCB2*) as an estrogen-induced gene associated with breast carcinoma. (A) Scatter plot analysis of microarray data for 519 genes containing functional estrogen-responsive element in breast carcinomas comparing the recurrence and non-recurrence group ($n = 5$ in each group). Genes with an expression ratio, recurrence group to non-recurrence group, of more than 2.0 or <0.5 are located outside the diagonal line, and classified as group A or group B, respectively. Genes with a ratio between 2.0 and 0.5 were classified as group C. *NUCB2* showed the highest ratio in these genes (arrow). The right panel summarizes the gene list of group A. (B,C) Effects of estradiol on NUCB2 mRNA expression. MCF-7 cells were treated with indicated concentrations of estradiol with or without (–) ICI 182780 or tamoxifen for 3 days (B) or treated with estradiol (10 nM) for the indicated period (C). The relative NUCB2 mRNA level summarized as a ratio (%) compared with the basal level (non-treatment). Data are presented as the mean ± SD ($n = 3$). *$P < 0.05$ and ***$P < 0.001$ versus non-treatment (left bar) (B) or 0 h (left plot) (C).

histological grade, mitotic score, PR status, *HER2* status, or Ki-67 LI. The positive association between *NUCB2* status and lymph node metastasis was significant regardless of the ER status of these cases ($P = 0.02$) (Table S2). *NUCB2* status was positively associated with Ki-67 LI in the ER-positive group ($P = 0.02$), and was positively correlated with tumor size in ER-negative cases ($P = 0.03$).

When immunohistochemistry was carried out in ductal carcinoma *in situ*, *NUCB2* immunoreactivity was detected in the carcinoma cells (Fig. 2F) in 7 (32%) of 22 cases. The *NUCB2* positivity was 1.5-fold higher in invasive carcinoma (48%) than non-invasive carcinoma (32%), although it did not reach a level of significance ($P = 0.15$).

Association between *NUCB2* status and clinical outcome. In order to thoroughly examine the association between *NUCB2* status and patient prognosis, we excluded stage IV cases and used stage I–III breast carcinoma patients ($n = 141$) in the following analyses. As shown in Figure 3(A), *NUCB2* status was significantly associated with an increased incidence of recurrence ($P = 0.003$), and the multivariate analysis revealed that lymph node metastasis ($P = 0.01$), ER status ($P = 0.002$), and *NUCB2* status ($P = 0.001$) were independent prognostic factors for disease-free survival with relative risks over 1.0 (Table 2).

A breast cancer-specific survival curve of the patients is summarized in Figure 3(B); a significant correlation ($P = 0.0002$) was detected between *NUCB2* status and adverse clinical outcome in the 141 breast carcinoma patients examined. In the univariate analysis (Table 2), lymph node metastasis ($P = 0.0004$), *NUCB2* status ($P = 0.002$), ER status ($P = 0.003$), histological grade ($P = 0.01$), *HER2* status ($P = 0.01$), and tumor size ($P = 0.02$) were all indicated as significant prognostic variables for breast cancer-specific survival. A following multivariate analysis showed that only *NUCB2* status ($P = 0.0004$) and ER status ($P = 0.01$) were independent prognostic factors with a relative risk over 1.0, whereas lymph node metastasis

doi: 10.1111/j.1349-7006.2011.02119.x

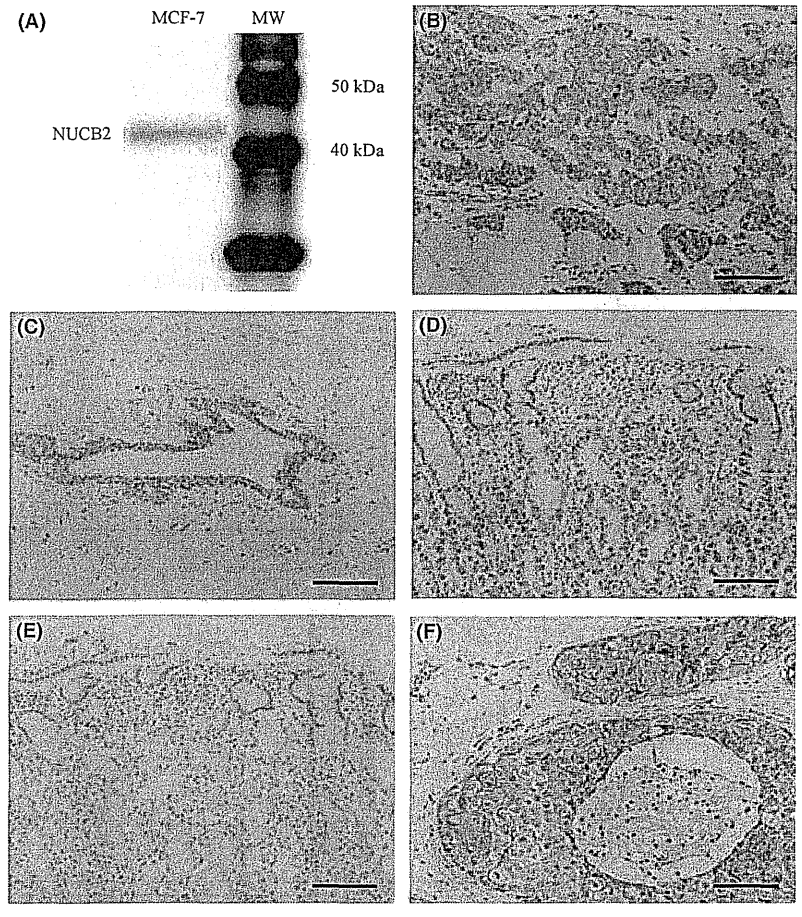

Fig. 2. Immunohistochemistry for nucleobindin 2 (*NUCB2*) in breast carcinoma. (A) Immunoblotting for *NUCB2* in MCF-7 cells. MW, molecular weight. (B) *NUCB2* immunoreactivity was detected in the carcinoma cells of invasive ductal carcinoma. (C) *NUCB2* immunoreactivity was weakly and focally detected in morphologically normal mammary glands. (D) Positive control section of *NUCB2* immunohistochemistry (gastric mucosa). (E) Negative control section of *NUCB2* immunohistochemistry (same area as Fig. 2D). (F) *NUCB2* immunoreactivity was detected in the carcinoma cells of ductal carcinoma *in situ*. Bar = 100 μm.

($P = 0.22$), histological grade ($P = 0.28$), *HER2* status ($P = 0.60$), and tumor size ($P = 0.07$) were not significant.

A similar association between *NUCB2* and worse prognosis was detected regardless of the Ki-67 status ($P = 0.03$ in cases with Ki-67 LI $\geq$ 10% and $P = 0.04$ in cases with Ki-67 < 10% for disease-free survival [Fig. 3C]; $P = 0.004$ in cases with Ki-67 LI $\geq$ 10% and *P*-value not available cases with Ki-67 < 10% because no patient died in the *NUCB2*-negative group for breast cancer-specific survival). When the 66 *NUCB2*-positive cases were further categorized into two groups according to immunointensity (++, strongly positive [$n = 16$]; +, modestly positive [$n = 50$]), no significant difference was detected between these two groups ($P = 0.60$ for disease-free survival [Fig. 3D], and $P = 0.49$ for breast cancer-specific survival).

Forty patients with stage I–III disease received tamoxifen therapy following surgery as an adjuvant treatment, and these cases were all positive for ER. *NUCB2* status was also markedly associated with an increased risk of recurrence (Fig. 3E) and worse prognosis (data not shown) in the patients who received tamoxifen therapy, although *P*-values were not available because no patient had recurrent disease or died in the group of *NUCB2*-negative cases. Significant association between *NUCB2* status and patients' clinical outcome was also detected in the 113 patients who received adjuvant chemotherapy ($P = 0.03$ for disease-free and $P = 0.002$ for breast cancer-specific survival), 38 ER-negative cases ($P = 0.0001$ for disease-free and $P < 0.0001$ for breast cancer-specific survival), or 24 cases with ER LI < 1% ($P = 0.001$ for disease-free [Fig. 3F] and $P = 0.0004$ for breast cancer-specific survival).

Effects of *NUCB2* expression on cell proliferation and invasion in breast carcinoma cells. The results of our study suggest that *NUCB2* is associated with worse prognosis of breast carcinoma patients regardless of their ER status, although *NUCB2* expression is upregulated by estrogen. In order to further examine the biological functions of *NUCB2* in human breast carcinoma, we transfected specific siRNA for *NUCB2* both in ER-positive MCF-7 and ER-negative SK-BR-3 breast carcinoma cells. The NUCB2 mRNA expression level was markedly decreased in these cells transfected with specific *NUCB2* siRNA (si1 or si2) at 3 days after transfection compared to cells transfected with control siRNA (siC). The ratio of NUCB2 mRNA level compared to that in the control siRNA was: MCF-7, 5% (si1) and 8% (si2); and SK-BR-3, 11% (si1) and 12% (si2).

As shown in Figure 4(A), the number of cells was significantly lower in MCF-7 cells transfected with *NUCB2* siRNA ($P < 0.001$ and 0.52-fold in si1, and $P < 0.001$ and 0.64-fold in si2) than in control cells transfected with siC 3 days after the transfection. A similar association was also detected in SK-BR-3 cells under the same conditions ($P < 0.001$ and 0.75-fold in si1, and $P < 0.001$ and 0.81-fold in si2). Figure 4(B) shows the

Table 1. Association between nucleobindin 2 (*NUCB2*) immunohistochemical status and clinicopathological parameters in 161 breast carcinomas

	NUCB2 status		*P*-value
	Positive (n = 77)	Negative (n = 84)	
Age† (years)	53.9 ± 1.4	54.4 ± 1.2	0.770
Menopausal status (%)			
Premenopausal	31 (19)	35 (22)	0.860
Postmenopausal	46 (29)	49 (30)	
Stage (%)			
I	18 (11)	24 (15)	0.730
II	38 (24)	43 (27)	
III	10 (6)	8 (5)	
IV	11 (7)	9 (6)	
Tumor size† (cm)	3.4 ± 0.4	3.4 ± 0.4	0.990
Lymph node metastasis (%)			
Positive	41 (25)	26 (16)	**0.004**
Negative	36 (22)	58 (36)	
Histological grade (%)			
1 (well)	20 (12)	24 (15)	0.930
2 (moderate)	30 (19)	31 (19)	
3 (poor)	27 (17)	29 (18)	
Mitotic score (%)			
1 (low)	33 (20)	43 (27)	0.570
2 (moderate)	22 (14)	21 (13)	
3 (high)	22 (14)	20 (12)	
ER status (%)			
Positive	65 (40)	53 (33)	**0.002**
Negative	12 (7)	31 (19)	
PR status (%)			
Positive	55 (34)	51 (32)	0.150
Negative	22 (14)	33 (20)	
HER2 status (%)			
Positive	22 (14)	24 (15)	0.990
Negative	55 (34)	60 (37)	
Ki-67 LI† (%)	23.6 ± 1.8	21.1 ± 2.1	0.380

†Data are presented as the mean ± SEM. All other values represent the number of cases and percentage. ER, estrogen receptor; LI, labeling index; PR, progesterone receptor. *P*-values <0.05 were considered significant, indicated in bold.

results of the migration assay. The number of migrated cells was significantly lower in both MCF-7 cells ($P < 0.001$ and 0.11-fold in si1, and $P < 0.001$ and 0.43-fold in si2) and SK-BR-3 cells ($P < 0.001$ and 0.36-fold in si1, and $P < 0.001$ and 0.31-fold in si2) transfected with *NUCB2* siRNA than in those transfected with control siRNA at 1 day (MCF-7) or 2 days (SK-BR-3) after the transfection. Moreover, the number of invaded cells was also significantly lower in the cells transfected with *NUCB2* siRNA (MCF-7, $P < 0.05$ and 0.21-fold in si1 and $P < 0.05$ and 0.29-fold in si2; SK-BR-3, $P < 0.01$ and 0.66-fold in si1 and $P < 0.001$ and 0.47-fold in si2) (Fig. 4C,D).

Discussion

Gene expression profiling is an important method to predict the likelihood of recurrence of disease in breast cancer patients,[19] in addition to conventional clinical and histopathological examination. A multigene classifier associated with recurrence has been proposed for breast carcinoma patients by several research groups,[19–21] and molecular-based diagnostic systems have been developed, such as MammaPrint[22] and Oncotype DX,[23] as well as the genomic grade index.[24] However, the selected genes vary markedly between these diagnostic systems, which may be partly due to the fact that they use different platforms for the analysis of gene expression. In addition, the biological functions have remained largely unknown in a great majority of these genes. In our present study, the results of microarray analysis revealed 17 genes that are potentially associated with recurrence in ER-positive breast carcinoma patients (group A in Fig. 1A). Among these, *IGFBP5* (insulin-like growth factor-binding protein 5) was reported to play an important role in breast carcinoma metastasis,[25,26] and is included in MammaPrint. In addition, *TGFA* (transforming growth factor α), a member of the epidermal growth factor family, is well-known to be involved in cellular proliferation and carcinogenesis.[27] The kinetochore-bound protein kinase *BUB1* (budding uninhibited by benzimidazoles 1) is a possible link to tumorigenesis.[28] *NUCB2* showed the highest expression ratio in this study, but this gene has not been listed in any multigene classifiers predicting breast carcinoma recurrence, nor has it been examined in breast carcinoma, to the best of our knowledge.

In this study, we first showed that *NUCB2* immunoreactivity was detected in 48% of breast carcinoma cases, although levels were almost negligible in morphologically normal mammary glands. *NUCB2* is known to mainly express in key hypothalamic nuclei with proven roles in energy homeostasis.[9] Moreover, recent investigations have indicated that *NUCB2* is also expressed in various human peripheral tissues, including the stomach, pancreas, reproductive organs, and adipose tissues, with relevant metabolic functions, suggesting that *NUCB2* signaling might participate in adaptative responses and in the control of body functions gated by the state of energy reserves.[29] However, *NUCB2* expression in carcinoma has only been examined in the stomach; Kalnina *et al.*[15] reported that *NUCB2* immunoreactivity was not detected in carcinoma cells in 15 gastric carcinoma cases examined. The relatively wide distribution of *NUCB2* immunoreactivity in our present study suggests that *NUCB2* plays an important role in human breast carcinoma.

Bourdeau *et al.*[14] evaluated genome-wide identification of EREs in humans, and identified a functional ERE element at 8257 bp from the most upstream mRNA 5′-end of the *NUCB2* gene. In our present study, *NUCB2* immunohistochemical status was positively associated with ER status in breast carcinoma tissue, and NUCB2 mRNA was significantly upregulated by estradiol in MCF-7 cells through ER. Therefore, *NUCB2* is considered one of the estrogen-induced genes in breast carcinoma cells. Results of our present study also indicated the presence of *NUCB2* in 12 of 43 (28%) ER-negative breast carcinoma cases; it might be the case that *NUCB2* was induced by a low or undetectable level of ER in these cases. However, it is also true that estrogen-mediated induction of NUCB2 mRNA was relatively slow in MCF-7 cells in our time-course study (Fig. 1C), suggesting that *NUCB2* expression is, at least in a part, induced by secondary responses, although the half-life of mRNA is an important factor in determining how long it takes to detect a change in the mRNA level of a specific gene.[4] In addition, *NUCB2* is expressed in various human tissues not necessarily considered targets for estrogens, as described above.[29] Therefore, other factors than estrogens might be involved in the expression of *NUCB2* in breast carcinoma cells. No information is currently available regarding the regulation mechanisms of *NUCB2* expression to the best of our knowledge, and further research is required.

Previous studies have shown that ICI 182780 possesses a greater ability to suppress estrogen-sensitive gene expression and greater antitumor activity than tamoxifen in breast carcinoma.[30] This is partly due to the fact that ICI 182780 does not have agonistic ER activity and reduces steady-state levels of ER by increasing the turnover of the protein, whereas tamoxifen does possess partial agonistic ER activity.[31] In our study, ICI 182780 was superior to tamoxifen in suppressing estradiol-mediated induction of NUCB2 mRNA in MCF-7 cells (Fig. 1B), which is consistent with previous studies.

doi: 10.1111/j.1349-7006.2011.02119.x

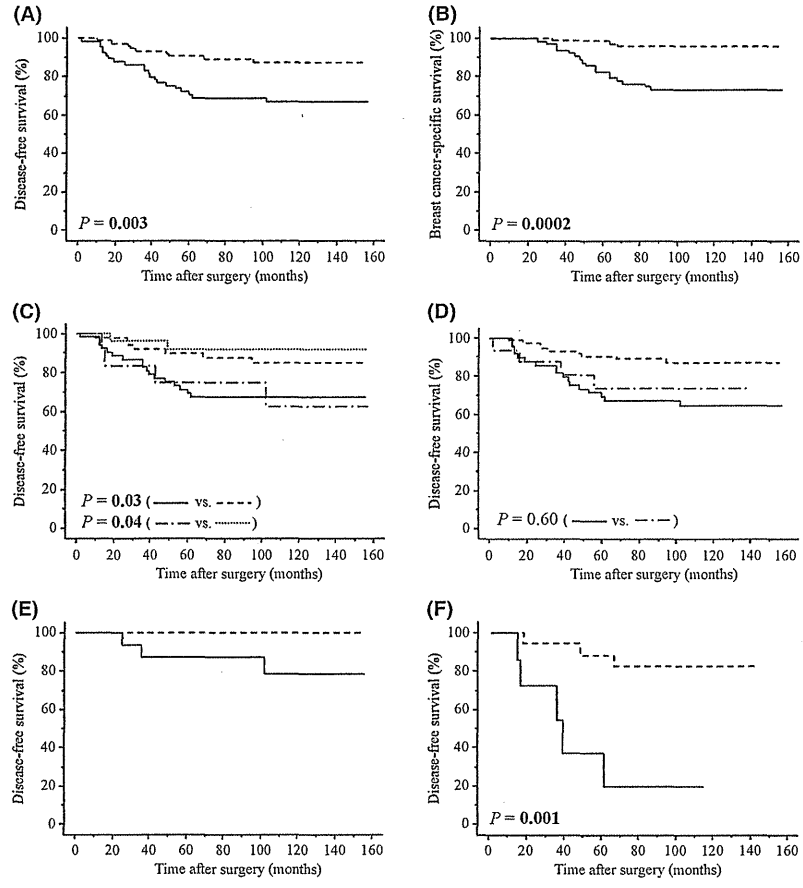

Fig. 3. Disease-free and breast cancer-specific survival of 141 breast carcinoma patients according to nucleobindin 2 (*NUCB2*) status. (A,B) *NUCB2* status was significantly associated with an increased risk of recurrence ($P = 0.003$) (A) and worse prognosis ($P = 0.0002$) (B). Solid line, positive for *NUCB2* ($n = 66$); dashed line, negative for *NUCB2* ($n = 75$). (C) Disease-free survival curve according to *NUCB2*/Ki-67 status. Solid line, positive for *NUCB2*/Ki-67 labeling index (LI) ≥ 10% ($n = 54$); dashed line, positive for *NUCB2*/Ki-67 LI < 10% ($n = 12$); dotted line, negative for *NUCB2*/Ki-67 LI ≥ 10% ($n = 50$); dot-dashed line, negative for *NUCB2*/Ki-67 LI < 10% ($n = 25$). (D) Disease-free survival curve according to *NUCB2* immunointensity. Solid line, strongly positive ($n = 16$); dashed line, modestly positive ($n = 50$); dot-dashed line, negative ($n = 75$). (E) *NUCB2* status was associated with recurrence in 40 patients who received tamoxifen therapy. *P*-value not available as there were no patients with recurrent disease in the *NUCB2*-negative group. Solid line, positive for *NUCB2* ($n = 16$); dashed line, negative for *NUCB2* ($n = 24$). (F) *NUCB2* status was significantly ($P = 0.001$) associated with recurrence in a group with estrogen receptor labeling index < 1% ($n = 24$). Solid line, positive for *NUCB2* ($n = 7$); dashed line, negative for *NUCB2* ($n = 17$).

In our present study, *NUCB2* immunoreactivity was positively associated with the presence of lymph node metastasis in breast carcinoma tissue both in ER-positive and ER-negative cases. In addition, subsequent *in vitro* studies indicated that both MCF-7 and SK-BR-3 cells transfected with siRNA *NUCB2* significantly decreased cell proliferation, and migration and invasion properties. Metastasis is considered as the major cause of treatment failure and death of carcinoma patients. It is a multistep process that involves migration and invasion of carcinoma cells, lymphogenous and/or hematogenous spread, and cell proliferation in the metastatic sites. Previous studies have shown that *NUCB2* has a wide variety of basic cellular functions, including an involvement in the energy homeostasis,[9] Ca^{2+} homeostasis,[8] and extracellular tumor necrosis factor receptor type 1 release,[10] although the biological functions have not yet been fully clarified. Results of our present study suggest that *NUCB2* plays a pivotal role, especially in the metastasis of breast carcinomas, and serve as a starting point for clarification of the biological roles of *NUCB2* in breast carcinoma. However, we could not necessarily detect a significant association between *NUCB2* status and mitotic score, Ki-67 LI, or invasion status in the clinical samples. Therefore, other factors might also play important roles in the processes of proliferation and invasion in breast carcinoma tissues.

In our present study, *NUCB2* status was also significantly associated with recurrence and worse prognosis in breast carcinoma patients, and a similar tendency was also detected in ER-positive patients who received tamoxifen therapy, or in ER-negative cases. In addition, results of multivariate analyses showed that *NUCB2* status was indeed an independent prognostic factor for both recurrence and breast cancer-specific survival. Results of our *in vitro* study indicated that tamoxifen inhibited estradiol-mediated induction of *NUCB2* expression in MCF-7 cells, but the basal expression level of NUCB2 mRNA still remained. Considering that the *NUCB2* expression level was the highest among the genes predominantly expressed in the recurrence group despite tamoxifen therapy (group A in Fig. 1A), *NUCB2* status in breast carcinoma tissues at the time of surgery might reflect the basal level of *NUCB2* as well as the level induced by estrogens in breast carcinoma cases. Therefore, residual carcinoma cells following surgical treatment in *NUCB2*-positive breast carcinomas could still have the potential to rapidly grow and/or metastasize,

Table 2. **Univariate and multivariate analyses of disease-free survival and breast cancer-specific survival in patients with stage I–III breast cancer (n = 141)**

Variable	Univariate	Multivariate	
	P-value	*P*-value	Relative risk (95% CI)
Disease-free survival			
Lymph node metastasis (positive/negative)	**<0.0001**	**0.0100**	3.1 (1.3–7.6)
ER status (negative/positive)	**0.0020**	**0.0020**	4.8 (1.8–13.0)
NUCB2 status (positive/negative)	**0.0100**	**0.0010**	4.6 (1.8–11.4)
HER2 status (positive/negative)	**0.0100**	0.6600	ND
Tumor size (≥2.0 cm/<2.0 cm)	**0.0200**	0.1300	ND
Histological grade (3/1, 2)	0.0900	ND	ND
Ki-67 LI (≥10%/<10%)	0.3500	ND	ND
Menopausal status (pre/post)	0.6400	ND	ND
Breast cancer-specific survival			
Lymph node metastasis (positive/negative)	**0.0004**	0.2200	ND
NUCB2 status (positive/negative)	**0.0020**	**0.0004**	12.0 (3.0–47.7)
ER status (negative/positive)	**0.0030**	**0.0100**	5.6 (1.5–20.7)
Histological grade (3/1,2)	**0.0100**	0.2800	ND
HER2 status (positive/negative)	**0.0100**	0.6000	ND
Tumor size (≥2.0 cm/<2.0 cm)	**0.0200**	0.0700	ND
Ki-67 LI (≥10%/<10%)	0.1000	ND	ND
Menopausal status (post/pre)	0.7800	ND	ND

Data considered significant ($P < 0.05$) in the univariate analyses are shown in bold, and were examined in the multivariate analyses.
CI, confidence interval; ER, estrogen receptor; LI, labeling index; ND, not done; *NUCB2*, nucleobindin 2; PR, progesterone receptor.

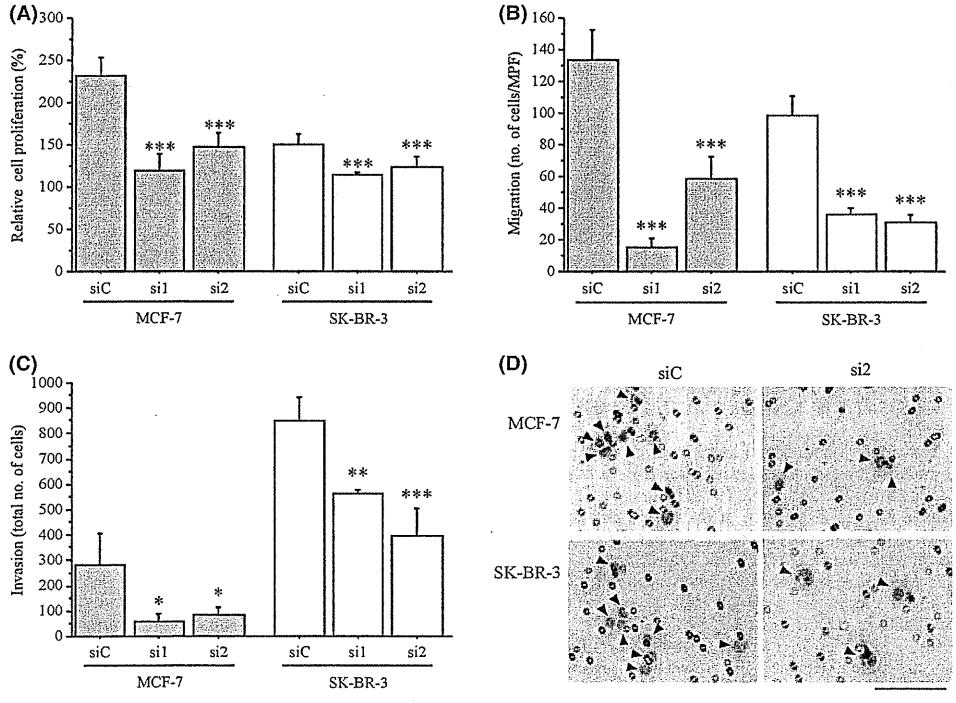

Fig. 4. Effects of nucleobindin 2 (*NUCB2*) on proliferation (A), and migration (B) and invasion (C,D) properties in breast carcinoma cells. (A–C) MCF-7 (gray bar) and SK-BR-3 (open bar) were transfected with *NUCB2*-specific siRNA (si1, si2) or control siRNA (siC). The relative cell proliferation was evaluated as a ratio (%) compared to that at 0 day after treatment (A). Migration ability was evaluated as an average number of cells in five middle power fields (MPF) (×200) on the lower surface of the membrane (B). Invasion ability was evaluated as the total number of cells (C). Data are presented as the mean ± SD (n = 6 [A]; n = 3 [B,C]). $^*P < 0.05$; $^{**}P < 0.01$; $^{***}P < 0.001$ versus control cells (left bar). (D) Representative microphotographs of results of invasion assay. Invaded carcinoma cells (arrows) were observed with 8 μm-sized pore. Nucleii stained with hematoxylin. When MCF-7 (upper panel) and SK-BR-3 (lower panel) cells were transfected with *NUCB2*-specific siRNA (si2) (right panel), the number of invading cells was decreased compared to the corresponding control (transfection with control siRNA [siC], left panel). Bar = 100 μm.

despite the fact that tamoxifen therapy partially suppresses the *NUCB2* expression level, thereby resulting in an increased recurrence and poor prognosis in these patients.

In summary, *NUCB2* was newly identified as a gene associated with recurrence in breast carcinoma patients by microarray analysis, and a subsequent *in vitro* study indicated that *NUCB2*

doi: 10.1111/j.1349-7006.2011.02119.x

expression was upregulated by estrogen in MCF-7 cells. *NUCB2* immunoreactivity was detected in 48% of breast carcinoma tissues, and was an independent prognostic factor of the patients. Results of further *in vitro* studies showed that *NUCB2* significantly increased the proliferation activity, and migration and invasion properties both in MCF-7 and SK-BR-3 cells. These findings suggest that *NUCB2* plays an important role, especially in the metastasis of breast carcinoma, and *NUCB2* status in primary breast carcinoma is reasonably considered a potent prognostic factor.

Acknowledgments

We appreciate the skillful technical assistance of Mr. Katsuhiko Ono (Department of Anatomic Pathology, Tohoku University Graduate School of Medicine, Sendai, Japan). This work was partly supported by a Grant-in-Aid for Scientific Research from the Japanese Ministry of Education, Culture, Sports, Science and Technology.

Disclosure Statement

The authors have no conflicts of interest.

Abbreviations

ER	estrogen receptor
ERE	estrogen-responsive element
LI	labeling index
NUCB2	nucleobindin 2
PR	progesterone receptor

References

1 Jordan VC. Fourteenth Gaddum Memorial Lecture. A current view of tamoxifen for the treatment and prevention of breast cancer. *Br J Pharmacol* 1993; **110**: 507–17.
2 Ali S, Coombes RC. Endocrine-responsive breast cancer and strategies for combating resistance. *Nat Rev Cancer* 2002; **2**: 101–12.
3 Suzuki T, Inoue A, Miki Y *et al.* Early growth responsive gene 3 in human breast carcinoma: a regulator of estrogen-meditated invasion and a potent prognostic factor. *Endocr Relat Cancer* 2007; **14**: 279–92.
4 Frasor J, Danes JM, Komm B, Chang KC, Lyttle CR, Katzenellenbogen BS. Profiling of estrogen up- and down-regulated gene expression in human breast cancer cells: insights into gene networks and pathways underlying estrogenic control of proliferation and cell phenotype. *Endocrinology* 2003; **144**: 4562–74.
5 Hayashi SI, Eguchi H, Tanimoto K *et al.* The expression and function of estrogen receptor alpha and beta in human breast cancer and its clinical application. *Endocr Relat Cancer* 2003; **10**: 193–202.
6 Miura K, Titani K, Kurosawa Y, Kanai Y. Molecular cloning of nucleobindin, a novel DNA-binding protein that contains both a signal peptide and a leucine zipper structure. *Biochem Biophys Res Commun* 1992; **187**: 375–80.
7 Barnikol-Watanabe S, Gross NA, Götz H *et al.* Human protein NEFA, a novel DNA binding/EF-hand/leucine zipper protein. Molecular cloning and sequence analysis of the cDNA, isolation and characterization of the protein. *Biol Chem Hoppe Seyler* 1994; **375**: 497–512.
8 Taniguchi N, Taniura H, Niinobe M *et al.* The postmitotic growth suppressor necdin interacts with a calcium-binding protein (NEFA) in neuronal cytoplasm. *J Biol Chem* 2000; **275**: 31674–81.
9 Oh IS, Shimizu H, Satoh T *et al.* Identification of nesfatin-1 as a satiety molecule in the hypothalamus. *Nature* 2006; **443**: 709–12.
10 Islam A, Adamik B, Hawari FI *et al.* Extracellular TNFR1 release requires the calcium-dependent formation of a nucleobindin 2-ARTS-1 complex. *J Biol Chem* 2006; **281**: 6860–73.
11 Elston CW, Ellis IO. Pathological prognostic factors in breast-cancer. 1. The value of histological grade in breast-cancer -experience from a large study with long-term follow-up. *Histopathology* 1991; **19**: 403–10.
12 Miki Y, Suzuki T, Kitada K *et al.* Expression of the steroid and xenobiotic receptor and its possible target gene, organic anion transporting polypeptide-A, in human breast carcinoma. *Cancer Res* 2006; **66**: 535–42.
13 Nagasaki S, Suzuki T, Miki Y *et al.* 17Beta-hydroxysteroid dehydrogenase type 12 in human breast carcinoma: a prognostic factor via potential regulation of fatty acid synthesis. *Cancer Res* 2009; **69**: 1392–9.
14 Bourdeau V, Deschênes J, Me'tivier R *et al.* Genomewide identification of high-affinity estrogen response elements in human and mouse. *Mol Endocrinol* 2004; **18**: 1411–27.
15 Kalnina Z, Silina K, Bruvere R *et al.* Molecular characterisation and expression analysis of SEREX-defined antigen NUCB2 in gastric epithelium, gastritis and gastric cancer. *Eur J Histochem* 2009; **53**: 7–18.
16 Takagi K, Miki Y, Nagasaki S *et al.* Increased intratumoral androgens in human breast carcinoma following aromatase inhibitor exemestane treatment. *Endocr Relat Cancer* 2010; **17**: 415–30.
17 Oka K, Suzuki T, Onodera Y *et al.* Nudix-type motif 2 in human breast carcinoma: a potent prognostic factor associated with cell proliferation. *Int J Cancer* 2011; **128**: 1770–82.
18 Ramanjaneya M, Chen J, Brown JE *et al.* Identification of nesfatin-1 in human and murine adipose tissue: a novel depot-specific adipokine with increased levels in obesity. *Endocrinology* 2010; **151**: 3169–80.
19 Oh DS, Troester MA, Usary J *et al.* Estrogen-regulated genes predict survival in hormone receptor-positive breast cancers. *J Clin Oncol* 2006; **24**: 1656–64.
20 Huang E, Cheng SH, Dressman H *et al.* Gene expression predictors of breast cancer outcomes. *Lancet* 2003; **361**: 1590–6.
21 Naoi Y, Kishi K, Tanei T *et al.* Development of 95-gene classifier as a powerful predictor of recurrences in node-negative and ER-positive breast cancer patients. *Breast Cancer Res Treat* 2011; **128**: 633–41.
22 van't Veer LJ, Dai H, van de Vijver MJ *et al.* Gene expression profiling predicts clinical outcome of breast cancer. *Nature* 2002; **415**: 530–6.
23 Paik S. Development and clinical utility of a 21-gene recurrence score prognostic assay in patients with early breast cancer treated with tamoxifen. *Oncologist* 2007; **12**: 631–5.
24 Sotiriou C, Wirapati P, Loi S *et al.* Gene expression profiling in breast cancer: understanding the molecular basis of histologic grade to improve prognosis. *J Natl Cancer Inst* 2006; **98**: 262–72.
25 Hao X, Sun B, Hu L *et al.* Differential gene and protein expression in primary breast malignancies and their lymph node metastases as revealed by combined cDNA microarray and tissue microarray analysis. *Cancer* 2004; **100**: 1110–22.
26 Li X, Cao X, Li X, Zhang W, Feng Y. Expression level of insulin-like growth factor binding protein 5 mRNA is a prognostic factor for breast cancer. *Cancer Sci* 2007; **98**: 1592–6.
27 Booth BW, Smith GH. Roles of transforming growth factor-alpha in mammary development and disease. *Growth Factors* 2007; **25**: 227–35.
28 Klebig C, Korinth D, Meraldi P. Bub1 regulates chromosome segregation in a kinetochore-independent manner. *J Cell Biol* 2009; **185**: 841–58.
29 García-Galiano D, Navarro VM, Gaytan F, Tena-Sempere M. Expanding roles of NUCB2/nesfatin-1 in neuroendocrine regulation. *J Mol Endocrinol* 2010; **45**: 281–90.
30 Osborne CK, Coronado-Heinsohn EB, Hilsenbeck SG *et al.* Comparison of the effects of a pure steroidal antiestrogen with those of tamoxifen in a model of human breast cancer. *J Natl Cancer Inst* 1995; **87**: 746–50.
31 Dauvois S, White R, Parker MG. The antiestrogen ICI 182780 disrupts estrogen receptor nucleocytoplasmic shuttling. *J Cell Sci* 1993; **106**: 1377–88.

Supporting Information

Additional Supporting Information may be found in the online version of this article:

Table S1. Genes predominantly expressed in the non-recurrence group, classified as group B.

Table S2. Association between nucleobindin 2 (*NUCB2*) status and clinicopathological parameters according to estrogen receptor status in 161 breast carcinomas.

Please note: Wiley-Blackwell are not responsible for the content or functionality of any supporting materials supplied by the authors. Any queries (other than missing material) should be directed to the corresponding author for the article.

UICC
global cancer control

IJC
International Journal of Cancer

MicroRNA-34b functions as a potential tumor suppressor in endometrial serous adenocarcinoma

Eri Hiroki[1], Fumihiko Suzuki[1], Jun-ichi Akahira[2], Satoru Nagase[1], Kiyoshi Ito[1], Jun-ichi Sugawara[1], Yasuhiro Miki[3], Takashi Suzuki[3], Hironobu Sasano[3] and Nobuo Yaegashi[1]

[1] Department of Obstetrics and Gynecology, Tohoku University Graduate School of Medicine, Sendai, Japan
[2] Department of Pathology, Tohoku Kosei Nenkin Hospital, Sendai, Japan
[3] Department of Pathology, Tohoku University Graduate School of Medicine, Sendai, Japan

Endometrial serous adenocarcinoma (ESC) is aggressive and carries a poor prognosis. p53 is frequently mutated in ESC. microRNAs (miRNAs) are a direct p53 target and have been implicated in cancer cell behavior. In this study, we compared miRNA expression levels in ESC with the levels in endometrial endometrioid adenocarcinoma (EEC) and normal endometria. Six miRNAs were identified as having aberrant down-regulation specific to ESC with miR-34b being most pronounced. miR-34b was found to have promoter hypermethylation, which when reversed, restored miR-34b expression in the cell lines treated with 5-aza-2′ deoxycytidine (DAC). Ectopic expression of miR-34b in turn inhibited cell growth, migration and most notably invasion. Our findings suggest a relationship among p53 mutation, miR-34b promoter methylation and tumor cell behavior. These effects are likely mediated by the downstream target of miR-34b, the proto-oncogene mesenchymal-epithelial transition factor (MET), a known prognostic factor in endometrial carcinomas. The expression of MET was reduced following the restoration of miR-34b in cell lines. In summary, our data suggest that miR-34b plays a role in the molecular pathogenesis of endometrial cancer.

Introduction

Endometrial serous adenocarcinoma (ESC) accounts for 10% of all endometrial carcinomas. In contrast to the more common Type I endometrial carcinomas, this tumor often presents at an advanced stage with deep myometrial invasion and a high incidence of lymph node involvement. The average age of onset is older than for Type I endometrial carcinoma.[1] The recurrence rate for ESC is high and the 5-year survival rate ranges from 15 to 51%.[2] The prognosis of ESC is, at best, equivalent to that of Grade III endometrial endometrioid adenocarcinoma (EEC) confined to the uterus.[3] The most prominent genetic alteration in ESC, demonstrated in 90% of tumors, is p53 mutation,[4] which frequently manifests as an accumulation of defective p53 protein.[5,6] Although p53 mutation is a common genetic alteration in a variety of tumor types, its role in tumorigenesis, particularly in gynecologic cancers, has not been completely elucidated. Furthermore, conflict exists regarding the utilization of p53 alterations as a prognostic factor. It is plausible that cell context-specific differences in pathways downstream of p53 may also play a role.

Direct targets of p53 include DNA sequences coding for microRNAs (miRNAs). miRNAs are single-stranded, noncoding RNAs of 18–24 nucleotides which have recently been shown to regulate protein expression. miRNAs bind to specific mRNAs, thereby blocking translation and increasing degradation.[7] Several of these mRNA targets code for proteins with oncogene and tumor suppressor functions;[8,9] therefore, by affecting the translation of these genes, miRNAs may play a key role in cellular transformation[10,11] and tumor metastasis.[12]

Members of the miR-34 family (miR-34a, miR-34b and miR-34c) are direct miRNA targets of p53 and represent potential tumor suppressors.[13–18] Expression of these miRNAs appears to be epigenetically regulated. DNA methylation of miR-34b/c has been found in colorectal cancer as well as in melanoma, in which methylation of CpG islands correlates with decreased expression and increased metastatic potential.[19,20] This effect may be mediated by the MET proto-oncogene, which has been identified as a putative target gene of miR-34a.[14]

MET encodes the hepatocyte growth factor receptor, a tyrosine kinase that is associated with invasive ability, cell growth, angiogenesis and scattering.[21] Numerous studies have shown that invasive growth is attenuated by the inhibition of MET expression, indicating a close relationship between MET and invasive properties.[22,23] It is unclear, however, if MET plays a role in ESC.

Key words: microRNA, miR-34b, MET, endometrial cancer, serous
Additional Supporting Information may be found in the online version of this article.
DOI: 10.1002/ijc.27345
History: Received 23 Dec 2010; Accepted 28 Sep 2011; Online 2 Nov 2011
Correspondence to: Fumihiko Suzuki, Department of Obstetrics and Gynecology, Tohoku University Graduate School of Medicine, 1-1 Seiryo-Machi, Aoba-ku, Sendai 980-8574, Japan, Tel.: +81-22-717-7254, Fax: +81-22-717-7258, E-mail: suzuki62@med.tohoku.ac.jp

To investigate whether a relationship existed between miRNA and tumor behavior, we obtained miRNA profiles of endometrial carcinomas using an miRNA microarray. We then sought to identify specific miRNAs, and target mRNAs associated with invasiveness and p53 mutation in ESC. Finally, we investigated how these miRNAs affected the function of endometrial cancer cells.

Material and Methods

Cell lines

Four human endometrial cancer cell lines (Ishikawa, RL95-2, SPAC-1-L and USPC-1) were examined in this study. Ishikawa cells were provided by Dr. Nishida from the Department of Obstetrics and Gynecology, Institute of Clinical Medicine, University of Tsukuba (Ibaraki, Japan). RL95-2 cells were obtained from the American Type Culture Collection (Rockville, MD). Established human endometrial serous carcinoma cell lines were provided by the laboratory of Dr. Hirai (SPAC-1-L), Department of Gynecology, Cancer Institute Hospital (Tokyo, Japan)[24] and Dr. Santin (USPC-1), Department of Obstetrics and Gynecology, Division of Gynecologic Oncology at the Yale University School of Medicine (New Haven, CT).[25] All cell lines were cultured in the appropriate medium and passed at confluence on 10 cm^2 dishes (Becton Dickinson and Co., Lincoln Park, NJ). The dishes were cultured in a 37°C incubator supplied with humidified 5% CO_2 and 95% air. The medium was changed twice a week.

Cells were incubated in growth medium with or without the DNA demethylating agent, 1 μM 5-aza-2′ deoxycytidine (DAC; Sigma–Aldrich, St. Louis, MO), for 72 hr, replacing the drug and medium every 24 hr. For histone deacetylase inhibition, 0.5 μM trichostatin A (TSA; Sigma–Aldrich) was added for the final 16 hr.

Tissue samples

After obtaining informed consent, 21 serous adenocarcinoma tissues, 20 endometrioid adenocarcinoma tissues, and 7 normal endometrial tissues (four proliferative phases and three secretory phases) were retrieved from the surgical pathology files at Tohoku University Hospital (Sendai, Japan). The research protocol was approved by the Ethics Committee at Tohoku University Graduate School of Medicine (Sendai, Japan). All surgical specimens were collected between January 2001 and December 2006 at Tohoku University Hospital (Sendai, Japan). Only patients diagnosed with a pure adenocarcinoma without other histological elements were included. The clinical data and patient characteristics are shown in Supporting Information, Table S1. We also obtained control normal endometrial tissue samples from hysterectomy specimens obtained from patients who underwent surgery for benign conditions. No patients had received preoperative radiotherapy or chemotherapy. The lesions were classified using World Health Organization criteria and were staged according to the International Federation of Gynecology and Obstetrics system.[26,27] The specimens were processed in 10% formalin, fixed for 24–48 hr, paraffin embedded, and thin-sectioned (3 μm). Frozen archival specimens were embedded immediately upon collection in optimal cutting temperature (OCT) compound (Sakura Finetechnical, Tokyo, Japan) and stored at −80°C for further use. Only sections containing a minimum of 90% carcinoma by examination with hematoxylin–eosin staining were used for total RNA and DNA preparation. Total RNA, including miRNA, was extracted using QIAzol Lysis reagent (Qiagen, Valencia, CA) and the miRNeasy Mini Kit (Qiagen) according to the manufacturer's instructions. Genomic DNA was extracted using a QIAamp DNA Mini Kit (Qiagen).

Immunohistochemistry

Immunohistochemical analysis was performed with the streptavidin–biotin amplification method using a Histofine kit (Nichirei, Tokyo, Japan). A monoclonal antibody for p53 (B20.1) and a polyclonal antibody for MET (SP260) were purchased from Biomeda (Foster City, CA) and Santa Cruz Biotechnology, respectively. For immunostaining, the slides were heated in an autoclave at 121°C for 15 min for p53, and in a microwave for 20 min for MET in 0.01 M citric acid buffer following deparaffinization for antigen retrieval. The dilutions of primary antibodies for p53 and MET were 1:50 and 1:100, respectively. The antigen–antibody complex was visualized with 3,3′-diaminobenzidine solution and counterstained with hematoxylin. Tissue sections of colon cancer and breast cancer were used as positive controls for p53 and MET, respectively. For p53 expression, tumor cells were considered positive when more than 10% of the tumor cells showed nuclear staining. For MET expression, the distribution and intensity were scored according to methods which have been described previously.[28] The percentage of positive cells was classified as 0 (none), 1 (<1%), 2 (2–10%), 3 (11–33%), 4 (34–66%) and 5 (>67%). The immunointensity was classified as 0 (negative), 1 (very weak), 2 (weak), 3 (moderate), 4 (strong) and 5 (very strong). The total score of cell was obtained by adding the immunostaining score and the immunointensity score (range, 0–10). Scores from 2 to 10 were regarded as positive, whereas scores from 0 to 1 were regarded as negative. The immunohistochemical expression was independently reviewed by two of the authors (E. H. and J. A).

miRNA microarray analysis

RNA purity and concentration were confirmed using the Agilent 2100 Bioanalyzer (Agilent Technologies, Santa Clara, CA). miRNA microarrays were manufactured by Agilent Technologies and contained 20–40 features targeting each of 470 human miRNAs. Labeling and hybridization of total RNA samples (100 ng) were performed according to the manufacturer's protocol. The arrays were scanned with an Agilent microarray scanner (Agilent Technologies) using high dynamic range settings as specified by the manufacturer.